Journal of Structural Geology 92 (2016) 99–115

Contents lists available at ScienceDirect

Journal of Structural Geology

journal homepage: www.elsevier.com/locate/jsg

Structure and flow properties of syn-rift border faults: The interplay between fault damage and fault-related chemical alteration (Dombjerg Fault, Wollaston Forland, NE Greenland)

Thomas B. Kristensen [a, *], Atle Rotevatn [a], David C.P. Peacock [a], Gijs A. Henstra [a], Ivar Midtkandal [b], Sten-Andreas Grundvåg [c, 1]

[a] Department of Earth Science, University of Bergen, Allégaten 41, 5007 Bergen, Norway
[b] Department of Geosciences, University of Oslo, P.O. Box 1047, Blindern, 0316 Oslo, Norway
[c] Department of Arctic Geology, University Centre in Svalbard, P.O. Box 156, 9171 Longyearbyen, Norway

ARTICLE INFO

Article history:
Received 10 December 2015
Received in revised form
23 September 2016
Accepted 28 September 2016
Available online 29 September 2016

Keywords:
Syn-rift
Fault zone
Fault structure
Chemical alteration zone
Diagenesis

ABSTRACT

Structurally controlled, syn-rift, clastic depocentres are of economic interest as hydrocarbon reservoirs; understanding the structure of their bounding faults is of great relevance, e.g. in the assessment of fault-controlled hydrocarbon retention potential. Here we investigate the structure of the Dombjerg Fault Zone (Wollaston Forland, NE Greenland), a syn-rift border fault that juxtaposes syn-rift deep-water hanging-wall clastics against a footwall of crystalline basement. A series of discrete fault strands characterize the central fault zone, where discrete slip surfaces, fault rock assemblages and extreme fracturing are common. A chemical alteration zone (CAZ) of fault-related calcite cementation envelops the fault and places strong controls on the style of deformation, particularly in the hanging-wall. The hanging-wall damage zone includes faults, joints, veins and, outside the CAZ, disaggregation deformation bands. Footwall deformation includes faults, joints and veins. Our observations suggest that the CAZ formed during early-stage fault slip and imparted a mechanical control on later fault-related deformation. This study thus gives new insights to the structure of an exposed basin-bounding fault and highlights a spatiotemporal interplay between fault damage and chemical alteration, the latter of which is often underreported in fault studies. To better elucidate the structure, evolution and flow properties of faults (outcrop or subsurface), both fault damage *and* fault-related chemical alteration must be considered.
© 2016 The Author(s). Published by Elsevier Ltd. This is an open access article under the CC BY-NC-ND license (http://creativecommons.org/licenses/by-nc-nd/4.0/).

1. Introduction

Structurally controlled, half-graben basins in active rifts are controlled by basin-bounding faults that commonly juxtapose sandy hanging-wall deposits against a footwall of crystalline (igneous or metamorphic) 'basement' (Gawthorpe and Leeder, 2000, Fig. 1). In ancient rift basins, these rift-climax depocentres are commonly confined to the subsurface, buried under substantial late- and post-rift deposits. Exhumed, well-exposed examples of basin-bounding faults juxtaposing syn-rift clastics against crystalline 'basement' are rare. Some of the best-known examples occur in the Suez Rift, where Sharp et al. (2000) documented the structure and evolution of basin-bounding faults and their interaction with syn-rift sedimentation. Whereas many papers on the general structure of fault zones have been published (see review by Faulkner et al., 2010, and references therein), there are very few that document the structure of km-scale basin-bounding fault zones that juxtapose syn-rift clastic rocks against a footwall of crystalline rocks. In fact, the detailed structure within the damage zone of such faults has rarely, if ever, been studied in detail (Ord et al., 1988 being one notable exception). Furthermore, understanding the structure of such fault zones, which has strong implications for predicting their flow properties, is of great economic significance since many syn-rift hydrocarbon plays depend on lateral fault seal provided by their bounding faults (e.g. Spencer and Larsen, 1990). In addition, as Laubach et al. (2010) states, the relationship between deformation and chemical changes to sediments has received little attention. Motivated by the above points, the present study offers new insights into the structure of syn-rift basin-bounding faults by investigating a particularly well-exposed

* Corresponding author. University of Bergen, Department of Earth Science, PB 7803, N-5020 Bergen, Norway.
E-mail address: Thomas.Kristensen@uib.no (T.B. Kristensen).
[1] Now at: Department of Geology, University of Tromsø, Dramsveien 201, 9037 Tromsø, Norway.

http://dx.doi.org/10.1016/j.jsg.2016.09.012
0191-8141/© 2016 The Author(s). Published by Elsevier Ltd. This is an open access article under the CC BY-NC-ND license (http://creativecommons.org/licenses/by-nc-nd/4.0/).

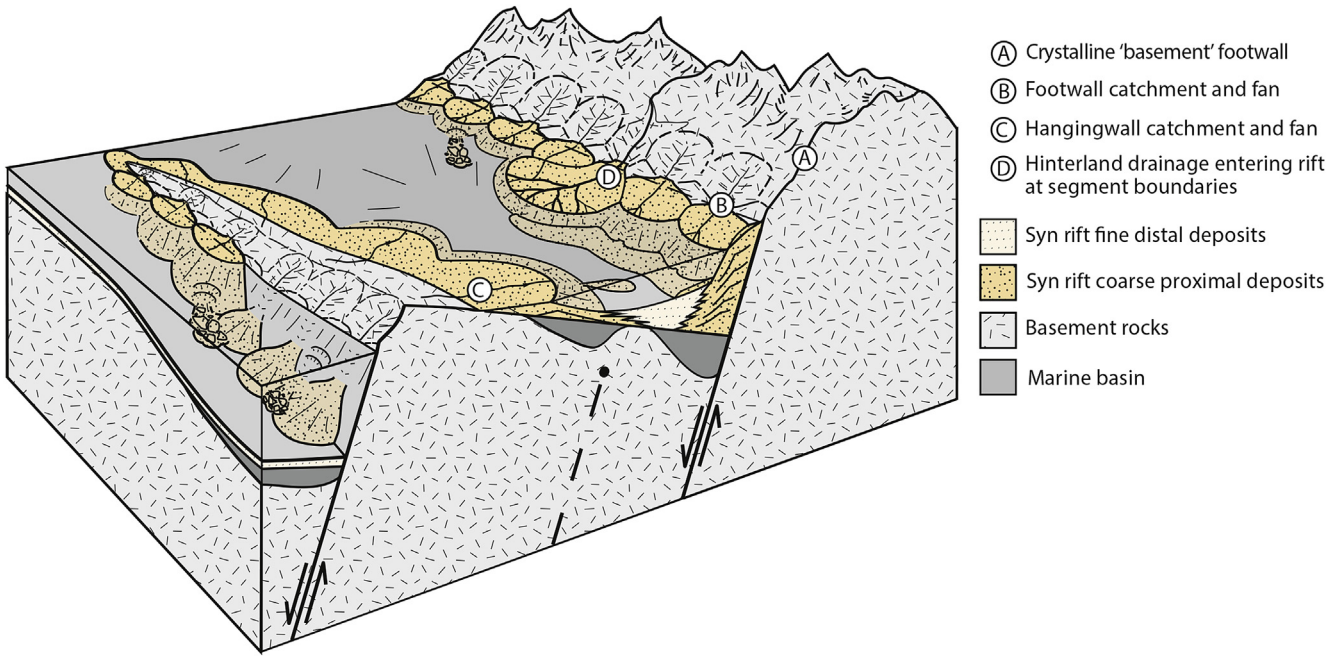

Fig. 1. Conceptual model for a structurally controlled, syn-rift, deep-marine, clastic depocentre in an active rift. Basin-bounding faults can juxtapose sandy hanging-wall reservoirs against footwall crystalline basement. Redrawn after Gawthorpe and Leeder (2000).

example, namely the Dombjerg Fault (Wollaston Forland, NE Greenland, Fig. 2), where syn-rift deep-water clastics in the hanging-wall are juxtaposed against crystalline basement in the footwall. The Dombjerg Fault, and the associated half-graben sedimentary fill of the Kuhn Block, provides excellent outcrops of footwall and hanging-wall damage zones, as well as the highly deformed central fault zone itself (*sensu* Childs et al., 2009; also termed 'fault core' by Caine et al., 1996).

Summarized, the aims of this study are therefore (i) to offer new insights into the structure of syn-rift border faults, and (ii) to provide a suitable analogue that may help reduce uncertainty in the prediction of flow-properties of such faults in the subsurface. The main aims are achieved through a set of specific objectives, which are to (i) document the detailed structure of the Dombjerg Fault and it's damage zone; (ii) elucidate the depth of deformation and the relative timing of different diagenetic and structural features in the damage zone; (iii) discuss implications for fault-controlled fluid flow and fluid-rock interaction, particularly in the context of hydrocarbon exploration. Comparison of the findings with subsurface examples imaged on seismic data illustrates the difficulty associated with understanding faults in such settings and their associated structures that are below seismic resolution.

Field data are used to qualitatively describe variations in structures as well as fault-related cementation (*sensu* Murray, 1960, i.e. pore-space reduction due to crystallization of secondary minerals in sedimentary rocks) and mineralization (*sensu* Fisher and Brantley, 1992, i.e. crystallization of minerals from fluids within a mechanically induced structure, such as faults and veins) backed up with quantitative data where possible. This is used to investigate the mutual interplay between structural/mechanical and diagenetic/chemical processes during faulting – an interplay that we would argue is often under-emphasized in fault zone studies in general.

2. Terminology

Fault structure has been the subject of numerous papers over the past decades, and we therefore find it useful to define the terminology used in this paper. First, we prefer the term fault *structure* over the term fault *architecture* for reasons laid out in Peacock (2008). Second, although the fault core and damage zone scheme developed by Caine et al. (1996) is widely used, Childs et al. (2009) present an alternative that, in our view is more useful in the description of the fault zone described herein. Largely following Childs et al. (2009), we use the term *fault zone* to describe the zone bounded by the outermost (on the hanging-wall *and* footwall side) principle synthetic slip-surfaces (same dip direction and sense of offset) that can be demonstrated at outcrop to be kinematically related and that each accommodate at least a few percent of the total offset (see Childs et al., 2009 for full discussion). The fault zone is also where the majority of fault slip is accommodated, localizing on the slip-surfaces. The term *fault rock* is used to describe gouge, breccias and cataclasites (e.g. Sibson, 1977). The term *fault strand* is used to describe any of the mentioned synthetic principle slip surfaces in the fault zone and its associated fault rock assemblage (Faulkner et al., 2010). *Damage zone* is the volume of deformed wall rocks around a fault surface that results from the initiation, propagation and build-up of slip along faults (Kim et al., 2004), whereas *relay zone* are zones of kinematic or geometric linkage between sub-parallel fault segments (*sensu* Fossen and Rotevatn, 2016).

3. Regional geological framework

East Greenland and its associated rifted passive margin record deformation related to a range of regional tectonic events, including: the Caledonian Orogeny in Middle Silurian to Early Devonian times (Gee et al., 2008) and subsequent orogenic collapse (Hartz et al., 2000; McClelland and Gilotti, 2003). This was followed by a period of episodic rifting during Late Palaeozoic to Mesozoic crustal thinning (Doré et al., 1999; Coward et al., 2003; Surlyk, 2003; Faleide et al., 2010) and subsequent Cenozoic breakup and onset of seafloor spreading leading to the opening of the North Atlantic (Dietz and Holden, 1970; Ziegler, 1988; Doré et al., 1999). In East Greenland, N-S trending fault systems separate the Caledonian

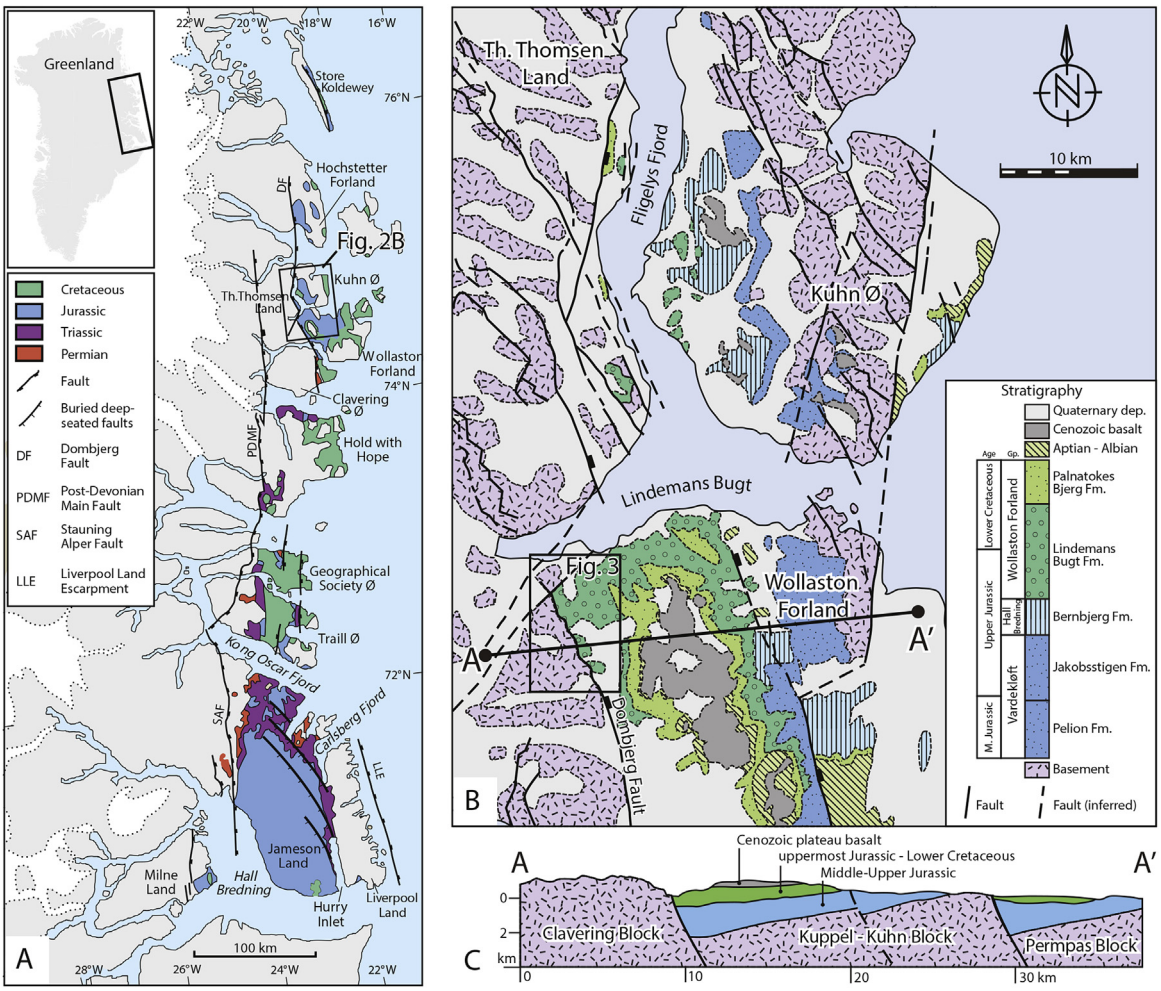

Fig. 2. Overview maps of the A) East Greenland Rift and B) the local structural setting in Wollaston Forland. C) Profile from A to A′ illustrating the east dipping faults with basement rocks in the footwall and Mesozoic siliciclastic basinal rocks in the hanging-wall. Redrawn from A) Surlyk (2003) and B) & C) Henstra et al. (2016).

basement to the west from the Paleozoic and Mesozoic rift basins to the east (Surlyk, 1978; Surlyk et al., 1986, 1981; Larsen, 1988; Kalsbeek, 1995) (Fig. 2A). These late Paleozoic to Mesozoic rift basins are generally referred to as the East Greenland rift system in the geological literature (e.g. Surlyk, 1990; Price et al., 1997). Strike-slip and extensional tectonics initiated in the Devonian and were followed by E-W-directed extension in the Mississippian to early Permian. Mesozoic rifting resulted in the formation of an N-S trending array of tilted fault blocks organized in a right-stepping en échelon pattern (Maync, 1947; Surlyk, 1978; Larsen, 1988; Surlyk and Korstgård, 2013). This fault array is expressed in Wollaston Forland by the c. 100 km long, E-dipping Clavering–Dombjerg –Thomsen Land Fault Zone, comprising alternating NNW-SSE and NNE-SSW oriented basin-bounding fault segments, along which the c. 10–20 km wide, W-tilted Kuhn Block half-graben is down-thrown (Fig. 2B and C).

Given the poly-phasal nature of the East Greenland rift system, Surlyk and Korstgård (2013) imply that this and other fault zones in the region may have been episodically active at least since the Carboniferous, and up to Cretaceous times. The studied Dombjerg Fault constitutes a 20–25 km long segment of this fault system with c. 3 km throw (Surlyk and Korstgård, 2013). Caledonian migmatite gneisses, pegmatites and amphibolites occur in the footwall of the Dombjerg Fault, whereas Middle Jurassic to Early Cretaceous syn-rift siliciclastics topped by Paleocene-Eocene volcanics are exposed in the immediate hanging-wall basin (Maync, 1947; Noe-Nygaard, 1976; Surlyk, 1978, 1984). During the Neogene, the Wollaston Forland area experienced several kilometres of uplift (Christiansen et al., 1992), which resulted in exhumation to the presently exposed level.

The hanging-wall siliciclastic basin fill in the study area were deposited during stages of i) early rifting in Bajocian to lower Volgian times (Surlyk and Korstgård, 2013), and ii) rift climax with formation of a c. 1 km deep depocentre in middle Volgian to late Ryazania times (Surlyk, 1984). The outcropping units in the hanging-wall of the Dombjerg Fault in the study area belong to the rift climax stage and consist of conglomerates and pebbly sandstones from sediment gravity-flow deposits sourced from the footwall scarp (Maync, 1947, 1949; Surlyk and Clemmensen, 1983; Surlyk, 1978, 1984; Surlyk and Korstgård, 2013). Henstra et al. (2016) propose that fine-grained material mainly entered the basin via a prominent south-facing relay ramp in the boundary fault system.

4. Field data

4.1. Overview of the Dombjerg Fault

The Dombjerg Fault trends NNW-SSE and dips c. 65° to the ENE. Overall, the fault is mostly straight in map view, but at the sub-km

scale the fault exhibits an undulating morphology along strike, following the topographic low of the Lindemansdalen valley (Fig. 3). The fault appears to tip-out northwards into a transfer zone, or basin-scale relay zone, across which there is a c. 8 km lateral graben step-over (*sensu* Fossen et al., 2010), and strain is transferred to the NE to the Thomsen Land Fault segment on the eastern shores of Thomas Thomsen Land.

In cross-section, the Dombjerg Fault is characterized by a c. 1 km wide damage zone that involves Caledonian migmatite gneisses, pegmatites and amphibolites in the footwall damage zone and Middle Jurassic to Early Cretaceous conglomerates and sandstones in the hanging-wall damage zone (Fig. 4). Towards the fault zone, the hanging-wall clastics are apparently tilted by c. 10–15° in contrast to the more horizontally bedded strata located further into the hanging-wall. This bedding angle correspond well to dips expected for the observed facies; i.e. deposits from accelerating gravity flows (suggesting a slope) as well as talus cones (Surlyk, 1978). Such geometries are also documented along other main boundary faults in the Jurassic rift of the northern North Atlantic (Ravnås and Steel, 1998). Thus we interpret this to be related to the depositional dip-architecture of the fault proximal clastic wedge rather than (frictional) drag along the Dombjerg Fault.

4.2. Host lithologies

The metamorphic basement footwall of the Dombjerg Fault in the study area is intensely affected by older deformation events, particularly related to the Caledonian Orogeny (Silurian-Devonian) (Gee et al., 2008), with asymmetric W-vergent folds representing the most prominent and common example of such deformation

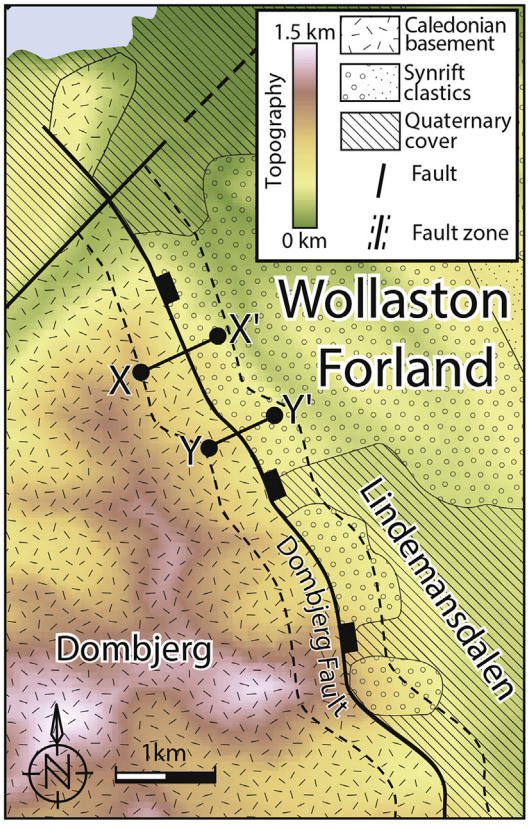

Fig. 3. Topographic map with structural elements displaying the juxtaposition of basement footwall rocks and hanging-wall basinal clastics. Position of transect X-X′ (Fig. 9) and Y-Y′ (Fig. 10) are indicated.

(Fig. 4). The footwall in the northern part of the study area is characterized by felsic gneisses, whereas in the southern part, mafic and ultramafic rocks are also common.

The hanging-wall deposits in the study area represent subaqueous gravity flow deposits sourced from the footwall, and the resulting lithologies include conglomerates and medium- to coarse-grained sandstones (Henstra et al., 2016). Interbeds of finer-grained sand and silt rarely occur. The conglomerate and sandstone clasts and grains are comprised predominantly of a combination of basement rock fragments and quartz grains.

4.3. Chemical alteration zone

The Dombjerg Fault is characterized by a chemical alteration zone (CAZ) (*sensu* Sutherland et al., 2012) where pervasive calcite cementation and mineralization affects the footwall and hanging-wall rocks in a zone extending a few hundreds of metres (and in some places up to 1 km) away from the fault zone. The width of the zone varies along strike and in the footwall the zone is demarcated by the existence of calcite veins. In the hanging-wall syn-rift clastics within the CAZ, calcite cement pervasively fills the pore space of the conglomerates and sandstones, leaving the rocks with negligible porosity (e.g. pervasive calcite cement in Fig. 5C and D). The cemented rocks in the hanging-wall stand out from the general appearance of the surrounding sedimentary rocks by their brown colour whilst the non-cemented equivalents have a warmer yellow-brown colouring. All the observed and sampled veins (8 samples) were interpreted to be calcite, both in the footwall (4 samples) and in the hanging-wall (4 samples). Further away from the fault zone and into the basin, the sandstones and conglomerates are relatively poorly lithified. These samples were too friable for thin section preparation and detailed analysis, but their poor consolidation, softness and colour suggest that they are largely unaffected by the calcite cementation seen in the more fault-proximal strata. The exact range and limit of the CAZ is however difficult to determine.

4.4. Structural characterization of the fault zone

4.4.1. Footwall damage zone

The deformation envelope associated with the Dombjerg Fault extends ca. 600 m into the basement footwall. At this distance a transition from ‘intact’ Caledonized basement, to increasingly faulted, jointed and brecciated rocks towards the fault zone mark the boundary between the footwall and the surrounding protolith. The damage zone in the footwall comprises veins (Fig. 6A), joints and minor faults (Fig. 6B).

Minor faults, oriented parallel to subparallel to the fault zone, typically feature striations (Figs. 6B and 7), and exhibit offsets in the range of centimetres to metres with little to no associated fault rock. Calcite filled veins (Figs. 5A and B; 6A) are frequently observed and range in width from 0.1 mm (thin veins in Fig. 5A) to 40 mm (Fig. 6A). Joints, as exemplified in Fig. 6G, crosscut veins and are thus interpreted to be late structures. The joints have strike orientations sub-orthogonal to the fault zone, overprinting minor faults and veins; apertures are generally 1–3 mm but increase up to 30 mm near discrete strands of the Dombjerg Fault.

Discrete fault strands are distributed throughout the fault zone in the basement, i.e. the most central part of the fault zone (Fig. 4). Joint and vein intensities appear to generally increase from the outer boundary of the damage zone in the footwall towards the fault zone. Joint and vein intensities increase dramatically in the proximity of the discrete fault strands. The discrete fault strands are further described below. Veins in the basement rocks of the footwall damage zone are 1–40 mm wide and calcite-filled; the veins

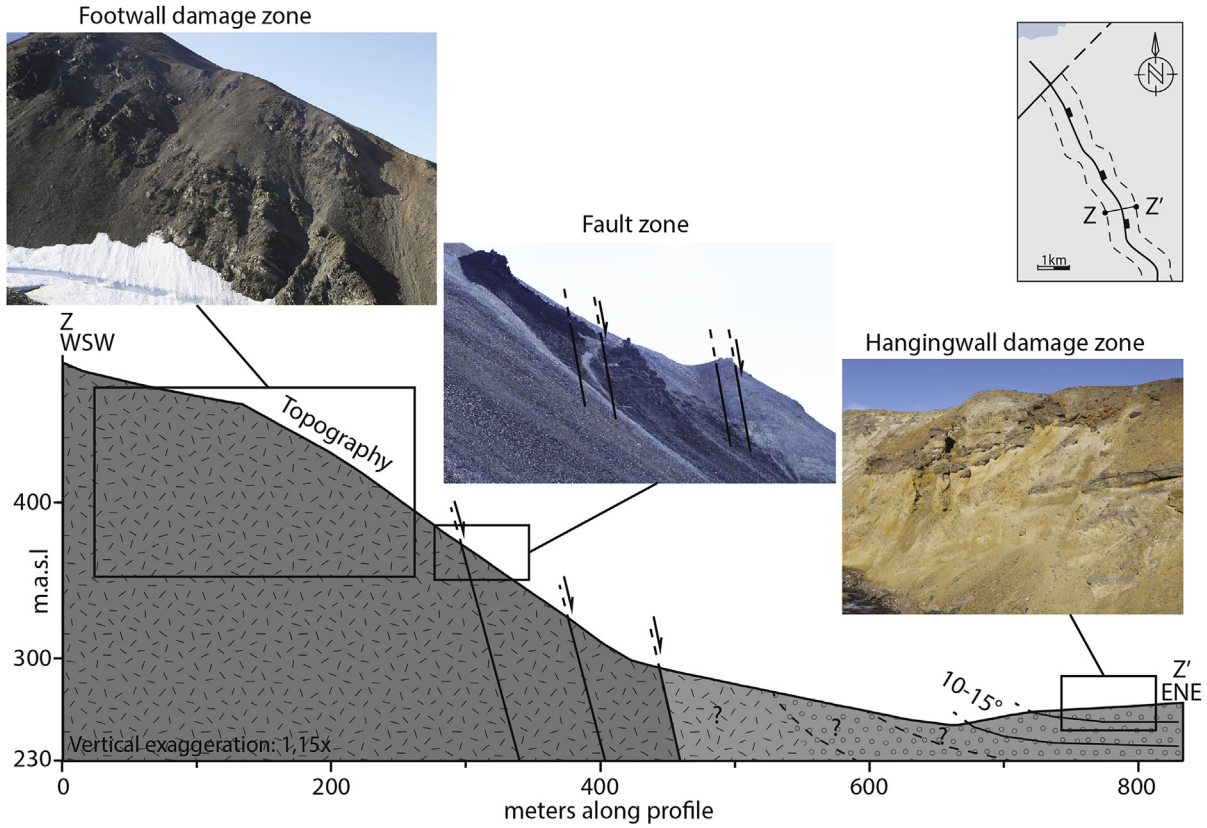

Fig. 4. Structural transect through the Dombjerg Fault illustrating the structural relationships and geometries between footwall crystalline rocks and sediment in the hanging-wall. Discrete fault strands occur in the fault zone as well as in the hanging-wall damage zone (in the basinal clastics). Note that the actual contact between hanging-wall and footwall rocks is not exposed at the surface and the exact contact is thus denoted with question marks.

commonly display multiple generations of fracture cement and have orientations sub-parallel to the fault zone (Fig. 7). Calcite diagenesis in the footwall damage zone appears pervasive, with calcite cement commonly found in grain-scale fractures.

4.4.2. Discrete fault strands and associated fault rock assemblages

Displacement on the Dombjerg Fault, which is proposed to have accumulated a maximum throw of 3 km to the base of the rift (Surlyk and Korstgård, 2013), is not localized onto a single principle slip surface. Slip appears to be distributed across several individual discrete fault strands within the c. 200 m wide fault zone. It is not possible to assess the amount of throw on each individual strand, but the intensity of brecciation and thickness of fault gouges (up to 50 cm) suggest the throw on each structure is significant, i.e. tens or hundreds of metres. All observable fault strands are localized in the basement part of the fault zone, whereas one or more fault strands is inferred in the zone of no exposure between the ENE-most basement outcrops and the WNW-most outcrops of basinal clastics. This zone of no exposure is c. 50–100 m wide and covered by debris and talus, indicating intense fracturing and weathering.

The fault strands show similar structures to each other and are characterized by assemblages of fault rock in an envelope of intensely veined, jointed and brecciated basement wall rocks. The fault rock assemblages include a central zone of fault gouge ranging in width from c. 5 cm–50 cm, commonly bounded by striated slip surfaces. Fault breccias occur adjacent to the central gouge zone. The fault breccias (classification following Woodcock and Mort, 2008) generally grade from crackle and mosaic breccias to chaotic breccias nearest to the fault strands (Fig. 8). The fault breccias are generally associated with secondary calcite mineralization (Fig. 5A and B). The wall rocks are associated with an apparent increase in the intensity of veins and joints in the proximity of the fault strands. The joint intensity increases to such an extreme degree that the wall rock in places appears as incohesive and uncemented crackle breccias.

4.4.3. Hanging-wall damage zone

The envelope of deformation extends approximately 500 m from the fault zone into the clastic deposits of the hanging-wall. At this distance, hanging-wall deformation has generally tapered off completely.

Within the calcite-cemented fault-proximal CAZ, the deformation of the basinal clastics is characterized by veins (Fig. 6F), joints and minor faults (e.g. displaced clast in Fig. 6D) generally oriented sub-orthogonal to the fault zone (Fig. 7). The veins are calcite-filled, and are generally 2–5 mm wide, but some are up to 50 mm wide. Joints consistently overprint veins, and are associated with apertures in the range of 1–2 mm. Minor faults are far less common, but where present they are mostly dip-slip, or rarely strike-slip, with offsets ranging from ~20 mm to ~100 mm.

The intensities of veins and joints increase towards the contact with the faulted basement (the contact itself is not exposed), but fracturing is far less intense than in the footwall. Generally, vein and joint intensities are both in the range of 2–7 per metre in the most fault-proximal sandstone and conglomerate outcrops. The highest intensities taper off quickly with distance from the fault, and drops to a vein spacing of several metres by about 100 m from the fault. Still, veins are common up to c. 500 m away from the fault.

Due to the variable width and undulose geometry of the CAZ associated with the fault, some of the clastic deposits in the damage

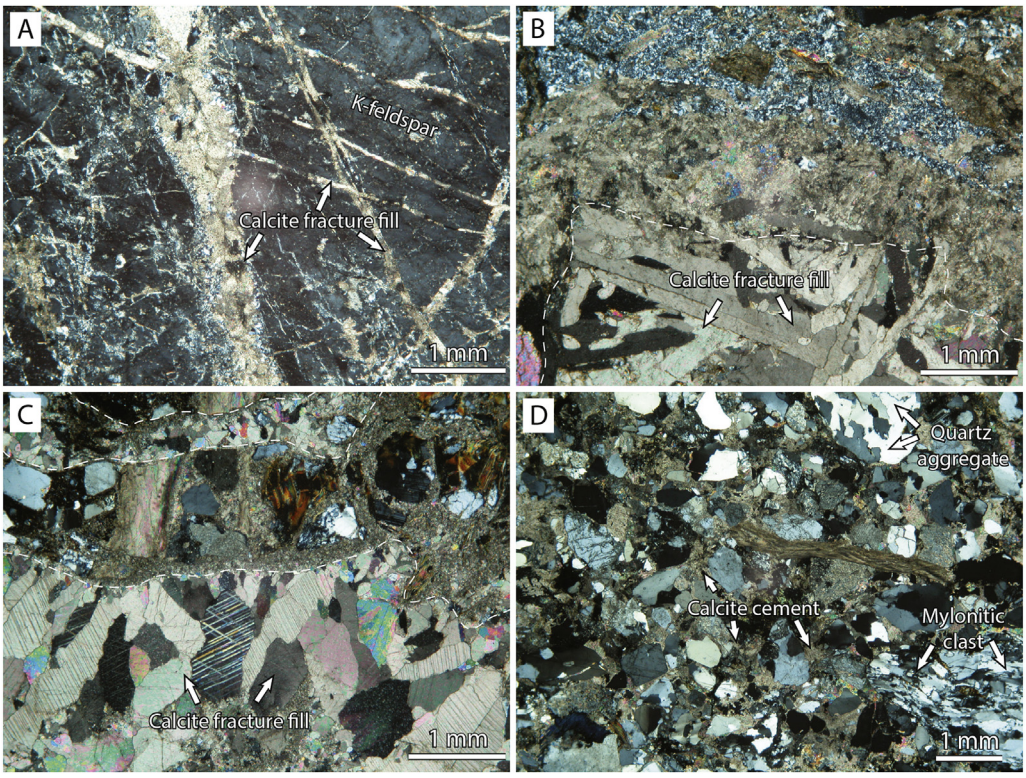

Fig. 5. Photomicrographs illustrating the variety of calcite cementation. A) Fracture fill in basement rocks displaying calcite filled fractures in a K-feldspar dominated host rock. B) Fracture fill in basement rocks. C) Fracture fill in basinal conglomerates close to point F in transect X-X′ (Fig. 9) with several zones indicating several generations of fracture fill. D) Calcite cementation in basin-fill conglomerates at the same locality as C) with varying clast assemblages and abundant calcite cement.

zone are not cemented. Here, deformation structures are predominantly disaggregational deformation bands (*sensu* Fossen et al., 2007) that form thin (1–5 mm), tabular zones of distributed shear in sandstones (Fig. 6C). Offsets are normal-sense and in the range of 2–50 mm. Thicker disaggregation zones (*sensu* Fisher and Knipe, 2001) are also common, with thicknesses up to 20 cm and normal offsets of up to 2 m. Thin section preparation was not possible because these uncemented deposits are highly friable.

4.5. Structural transects through the fault zone

Two structural transects have been made across the Dombjerg Fault to document the cross-sectional geometry and variability of the fault damage zone (X – X′ and Y – Y′ in Fig. 3). Significant scree cover on the steep slopes of Mount Dombjerg prevents the collection of continuous data along the transects, but data were collected where exposure allowed.

4.5.1. Transect A

Transect A is oriented WSW-ENE, from the outer part of the footwall damage zone, across the fault zone, and into the hanging-wall damage zone (X – X′ marks location for transect A in Fig. 3). The topographic profile, created based on elevation data in Google Earth, and images from the transect are shown in Fig. 9 (A–G). The profile is described from WSW towards ENE, i.e. from the footwall to the hanging-wall.

Point B is in the outer part of the footwall damage zone, where the folded, banded, felsic gneiss is relatively intact. The Caledonian W-vergent asymmetric folding is characteristic for the pre-existing structure of the basement, and formed at c. 400 Ma (Dallmeyer et al., 1994) at deep crustal levels under crystal-plastic conditions. The basement rocks here are absent of faults and only mildly affected by brittle deformation, with a small number of joints (approximately 4 per metre) and the occasional vein. Further into the footwall there are no indications of cementation or mineralization.

Joint frequencies increase rapidly ENE-wards from point B, and at point C, approximately 75 m towards the main fault trace, fracture frequencies range from 10 to over 50 joints per metre. The basement foliation is in places completely obliterated as the rock is disintegrated by brittle joints. Minor faults and larger discrete slip surfaces with slickenline lineations also occur in this area.

Points D and E are located in the fault zone itself, where discrete fault strands and fault rock assemblages occur. At point D, intense fracturing continues to characterize the host rocks, and fault breccias are associated with distributed minor faults. This breccia can be characterized as a mosaic to chaotic breccia, comprised of highly angular clasts of the basement host rock, cemented with calcite (Fig. 8). One of several discrete fault strands comprising the fault zone occurs at point E. The fault strand is a highly localized zone of deformation that appears to have accommodated major slip, and is associated with a fault rock assemblage that includes fault breccias and a c. 50 cm thick zone of fault gouge.

The coarse-grained sandstones and conglomerates in the hanging-wall at points F and G are pervasively cemented, and feature thick, abundant calcite veins up to 2 cm thick, as well as joints that crosscut the veins. Vein and joint intensities both reach 7 per metre in this area. Some discrete slip surfaces with subtle dip-slip striations/corrugations are found.

4.5.2. Transect B

Transect B extends ENE-wards from the fault zone within crystalline basement to the basinal clastics of the hanging-wall damage zone (Y – Y′ marks the location for transect B in Fig. 3).

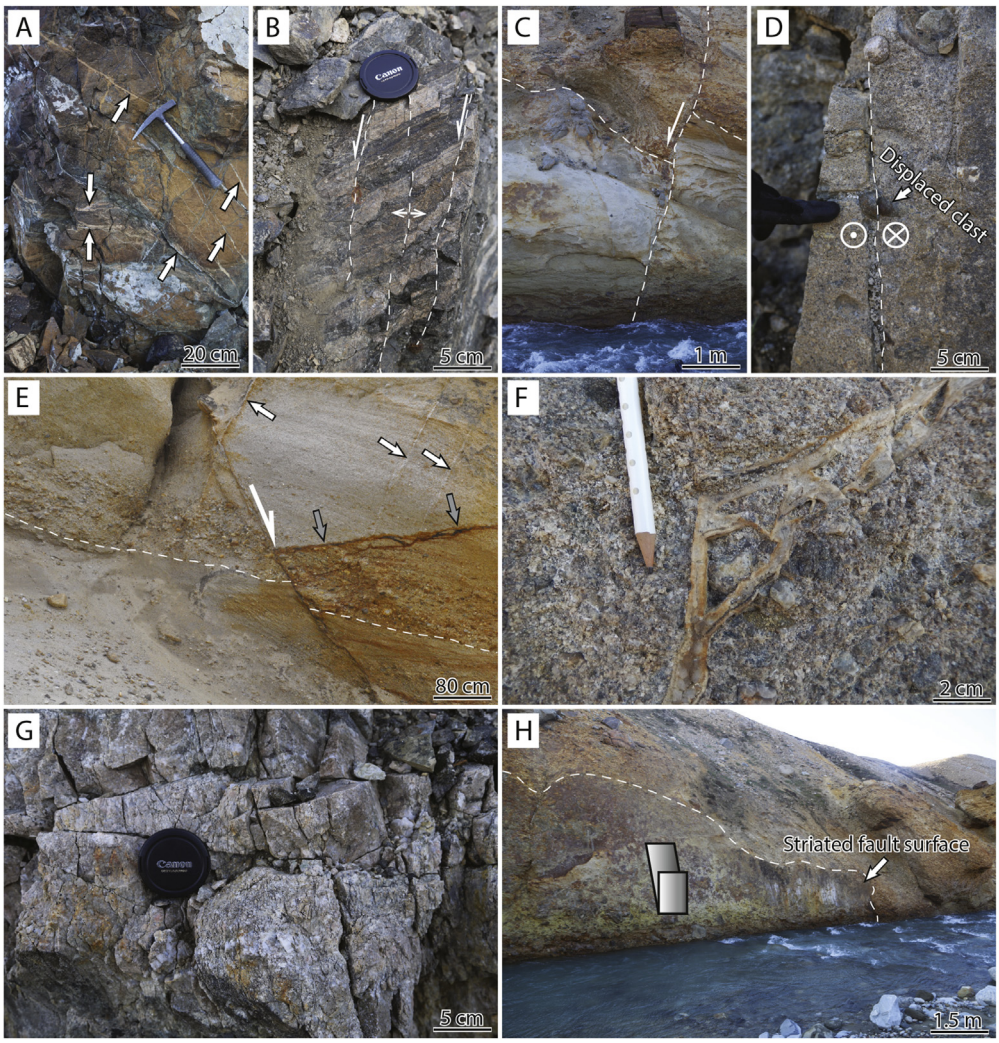

Fig. 6. Outcrop photographs displaying the variety in fracture types. A) Calcite-filled veins in brecciated basement rocks. B) Minor faults with c. 5–10 cm displacement and joints in Caledonian basement rocks near point B on transect X-X′ (Fig. 9). C) Disaggregation shear zone with c. 1 m displacement in basin fill rocks c. 500 m away from the fault zone. D) Strike-slip fault offsetting a conglomerate clast in the basin fill. E) Disaggregation shear band cluster with c. 50 cm aggregate displacement, c. 2 km basinward of the fault. F) Fracture with multigenerational calcite fill in conglomerates c. 200 m basinward of the fault. G) Intense brecciation and abundant joints in footwall basement rocks. H) Slip-surface with slickenlines in basin fill clastics c. 200 m basinward of the fault. Note the fault surface striations indicating dip-slip.

A topographic profile and images from the transect are shown in Fig. 10.

The transect starts (point B) at one of the discrete fault strands in the fault zone, within the footwall damage zone. The fault rocks associated with the discrete fault strand include fault gouge and fault breccias. The fault gouge is green to grey and occurs in a zone 20–30 cm wide, bounded by a discrete, striated slip surface on the hanging-wall side, and grading into, and partly mixed with, a fine-grained fault breccia on the footwall side. The hanging-wall side of the strand is comprised of banded felsic gneisses, whereas the footwall is comprised of mafic to ultramafic rocks containing olivine, serpentine and talc. Both footwall and hanging-wall of the strand are characterized by a high intensity of veins (20–30 per metre; Figs. 6A and 10B) and joints (>50 per metre).

Fault breccias are abundant in the immediate hanging-wall of this fault strand. The breccias mostly comprise calcite-cemented mosaic breccias. One such example occurs at Point C on the profile. This particular breccia is relatively fine-grained, with most clasts in the range of 2–4 mm (Fig. 10C).

The fault zone is comprised of 3 discrete fault strands and joint frequencies peak near these strands, but overall remains high throughout the fault zone. Point D is located c. 100 m from Point C in the direction of the main fault trace and approximately 40 m from the nearest fault strand in the fault zone. The crystalline rocks here are more intact and less obliterated by the fracturing, compared to the immediate wall rocks of the discrete fault strands. The rocks are still heavily jointed, however, with joint intensities in the range of 15–30 joints per metre.

The first outcrops of hanging-wall basinal clastics occur at Points E and F, approximately 75 m further ENE along the profile. The coarse-grained sandstones and conglomerates are also pervasively cemented here and as such are within the CAZ. The rocks are affected by veins, joints and minor faults. Large conglomerate clasts offset by minor faults are common (Fig. 10E). Vein frequencies are high, though lower than that of the footwall damage zone, with intensities of 2–10 veins per metre in the proximity of the fault zone. Joint intensities are similar, whilst minor faults exhibit a spacing of 2–5 m near the main fault. Veins are commonly 5–10 mm thick, but much thicker veins also occur, commonly where the veins occur along faults. At Point F, thick calcite cement (3 cm) occupies a releasing bend in a normal-sense fault. The cement shows calcite mineralization with growth fibres as

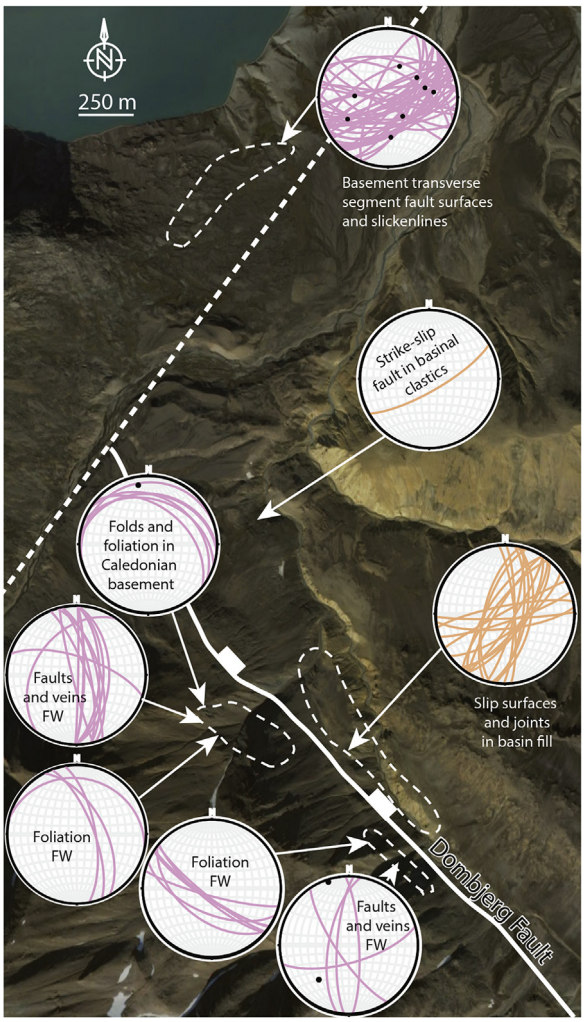

Fig. 7. Air photograph with equal-area lower-hemisphere projections of recorded veins, fractures and faults in the footwall (pink) and hanging-wall (orange) damage zone as well as orientations of folds and foliations in the Caledonian footwall protolith. (For interpretation of the references to colour in this figure legend, the reader is referred to the web version of this article.)

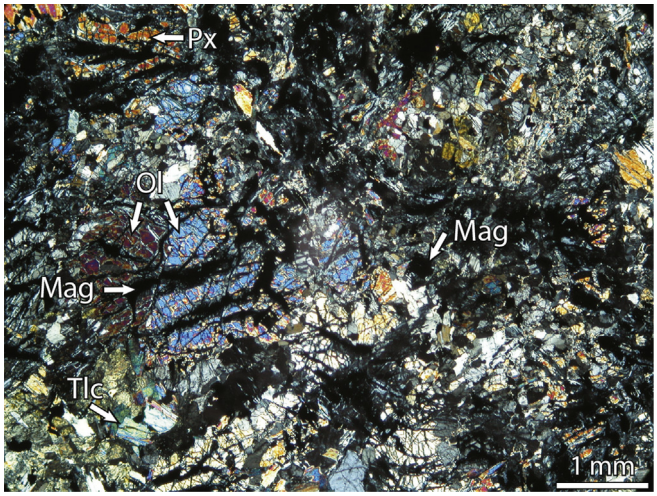

Fig. 8. Photomicrograph of a mosaic to chaotic breccia, comprised of highly angular clasts of the basement host rock, cemented with calcite close to point F in transect Y-Y′ (Fig. 10). The protolith of this sample is interpreted to be a peridotite and the minerals annotated in the figure are olivine (Ol), pyroxene (Px), magnetite (Mag) and talc (Tlc). RAMAN spectroscopy also identified chlorite and amphiboles in the sample.

evidence of syn-kinematic mineral growth that indicate the opening direction of the vein segment (e.g. Fig. 10G).

Minor faults are uncommon further away from the fault zone, and the intensities of veins and joints decrease. A few hundred metres away from the fault zone, and outboard of this transect, the CAZ ends and the rocks are unaffected by the pervasive cementation and mineralization seen closer to the fault. Thus, the sandstones and conglomerates are more loose and friable. Here, disaggregational deformation bands are found, and discrete fracturing is less common (Fig. 6E). A schematic cross-sectional summary of the observations laid out in Section 4 are presented in Fig. 11. This will be further treated in the discussion.

5. Discussion

The Dombjerg Fault at Wollaston Forland, NE Greenland, is an example of a basin-bounding border fault that juxtaposes crystalline rocks in its footwall against syn-rift deep-water clastics in its hanging-wall. Well-exposed examples are rare globally, and this study provides an important outcrop analogue for fault-trapped syn-rift hydrocarbon plays in rift basins.

Based on the syn-rift stratal expansion of the Late Jurassic-Early Cretaceous syn-rift succession as well as work by previous authors (Surlyk and Korstgård, 2013), the Dombjerg Fault was a syn-rift surface-breaching border fault in the Late Jurassic to Early Cretaceous, but was likely also active earlier during previous Paleozoic and Mesozoic tectonic phases (Surlyk and Korstgard, 2013). In the following we discuss this polyphasal syn-rift border fault in terms of its structure, timing/depth of deformation, and draw comparisons with subsurface examples. Finally, we discuss the implications for understanding the fluid flow properties and assessing the fault seal/leakage potential of such faults.

5.1. Fault zone structure

Fault zone descriptions have in recent years typically followed a scheme under which faults are divided into two domains, namely a fault core and a damage zone (e.g. Caine et al., 1996). According to this scheme, faults feature a fault core where the majority of fault slip is accommodated and is typically characterized by slip surfaces, gouge, cataclasites and breccias (e.g. Chester and Logan, 1986; Caine et al., 1996; Evans et al., 1997; Billi et al., 2003; Bastesen et al., 2009), surrounded by a damage zone, which is an envelope of fault-related subsidiary structures (veins, joints, deformation bands and small faults; Chester and Logan, 1986; Scholz, 2002; Caine et al., 1996, 2010; Knipe et al., 1998). There are two problems associated with this dominating model for fault zone structure that are highlighted by the present study:

(1) The Dombjerg Fault is comprised of a ca. 1 km wide damage zone (Figs. 9 and 10), including damage in both the footwall and hanging-wall of the fault. The fault zone (*sensu* Childs et al., 2009) itself is located centrally, in the footwall part of the damage envelope, where fault slip has been distributed and accommodated onto several discrete fault strands, or 'cores' (*sensu* Caine et al., 1996), that are associated with extensive fault rock assemblages. As such, the fault zone structure does not fit well with the simple scheme of a single fault core enveloped in a damage zone (e.g. Caine et al., 1996), because there are multiple discrete fault strands, or 'fault cores', and the overall fault structure is therefore best

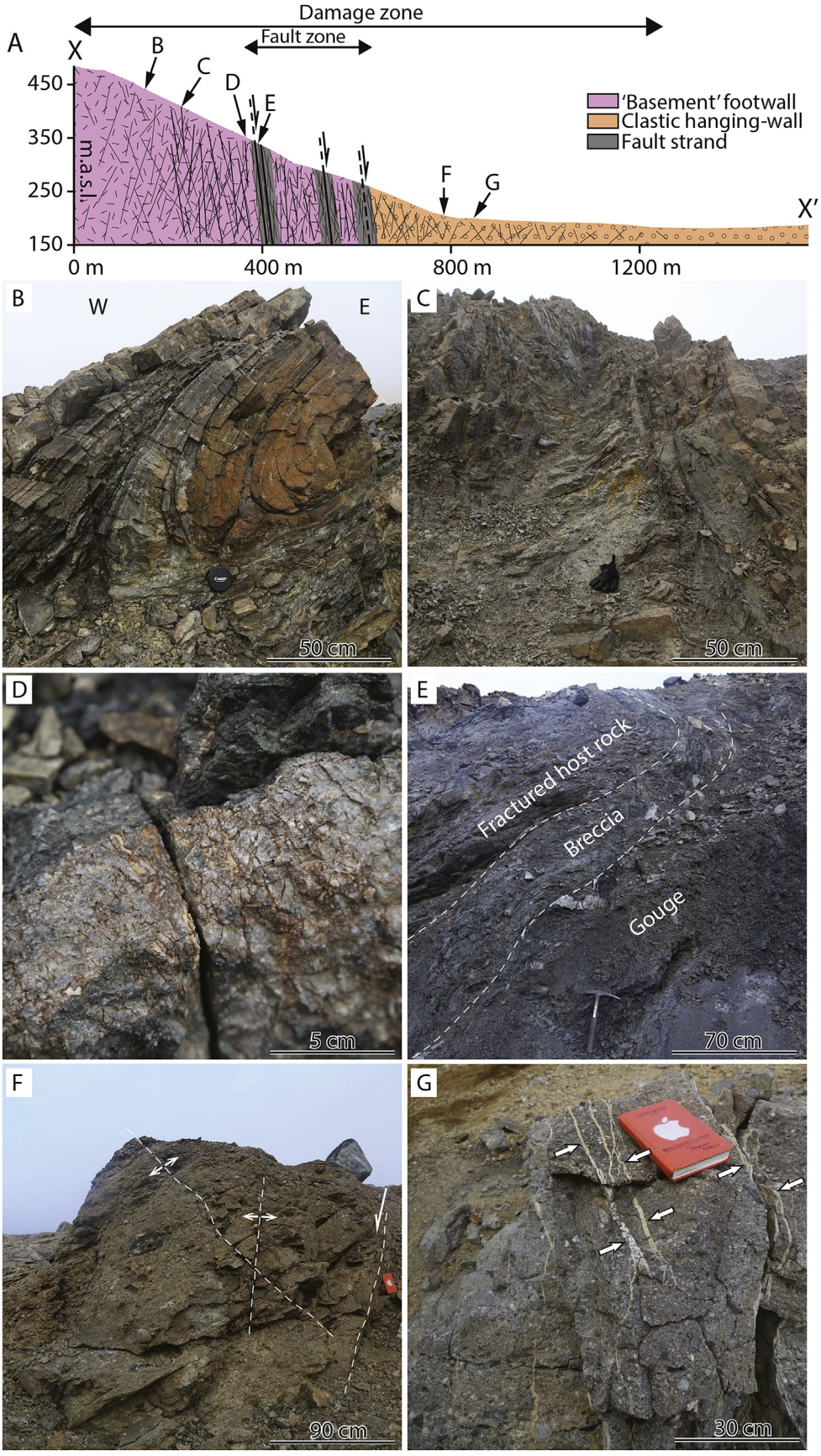

Fig. 9. Outcrop photopanel showing the variety of deformation found in transect A (marked X-X′ in Fig. 3) from footwall to hanging-wall across the fault zone proper. A) Transect topography and delineation of damage and central fault zone with marks for photograph localities. B) Caledonian W-vergent asymmetric fold in the footwall protolith. C) Intense footwall fracturing and brecciation. D) Intense brecciation and fracturing. E) Discrete fault strand with intense brecciation and a thick fault gouge in the fault zone. F) and G) Pervasively cemented basinal clastics in the hanging-wall, with abundant calcite veins.

described by a combination of the schemes presented by Childs et al. (1997, 2009) and Faulkner et al. (2003, 2010). A similar point was made by Michie et al. (2014), who cited Faulkner et al. (2003) and Childs et al. (1997) as the most all-encompassing models for fault zone geometries.

(2) In addition, the fault core and damage zone scheme may contribute to an over-emphasis on the relationship between structures and fault evolution, at the expense of the influence of cementation and mineralization. For example, significant work has been undertaken to understand how damage zone structure is linked to slip accumulation, and how it can be used to understand fault growth and evolution (e.g. Cowie and Shipton, 1998; Shipton and Cowie, 2001, 2003; Kim et al., 2003; De Joussineau and Aydin, 2007; Childs et al., 2009; Choi et al., 2016), whereas the role of chemical alteration during fault evolution is often under-emphasized (notable exceptions include Johansen et al., 2005; Tarasewicz et al., 2005; Woodcock et al., 2007, 2008; Sutherland et al., 2012; Gomila et al., 2016).

The Dombjerg Fault is characterized by extensive fault-related calcite cementation and mineralization and provides a telling example of the importance of understanding the relationship between chemical alteration and mechanical damage. Fault-related cementation and mineralization is a common feature globally (e.g. Knipe, 1992; Chan et al., 2000; Fodor et al., 2005) and reduces the porosity of sedimentary rocks and also mineralize fractures. As such, fault-related cementation and mineralization has an important influence on the evolution of faults. It is therefore problematic that the presently most commonly used nomenclature for fault zone description alludes to structural/mechanical damage, but does not emphasize terminology suited for the products of fault-controlled chemical/diagenetic fluid-rock interaction such as cementation and mineralization. Thus, it is our view that current fault zone terminology facilitates an under-reporting of the fault-related chemical alteration of rocks, and although the term 'alteration zone' have previously been used in some studies (Sutherland et al., 2012), its use has generally not been adopted in the wider literature on fault zone structure. We therefore suggest the term '*chemical alteration zone*' be included in schematic models for the fault zone structure and terminology (Fig. 12A–C) and defined as follows: the *CAZ* is a zone of fault-proximal cementation, mineralization (i.e. chemical alteration) of the protolith, facilitated by fluid flow in the *damage zone* of a fault. As such we differentiate two key components of fault zone structure: i) the damage zone, which encompasses damage related to the mechanical deformation of the protolith, e.g. faulting, fracturing and brecciation, and ii) the CAZ, which encompasses alteration caused by fault-related cementation and mineralization within the protolith.

5.2. Style, temperature, depth and relative timing of mechanical damage and chemical alteration

The distribution and style of deformation and fault-related mineralization forms a basis for discussing the temperature, depth and relative timing of the deformation associated with the Dombjerg Fault. The deformation is more intense in the footwall than in the hanging-wall (see Fig. 11). This may be explained by one or a combination of the following three factors. Firstly, the footwall consists of mechanically strong crystalline rocks in contrast to the mechanically weaker sedimentary strata of the hanging-wall. Secondly, the footwall may record deformation events that pre-date the age of the hanging-wall sediments, as suggested by the polyphasal nature of the Wollaston Forland Basin and the East Greenland rift system in general (Surlyk and Korstgård, 2013). The Late Jurassic to Early Cretaceous syn-rift hanging-wall strata have, given their age, only been subjected to the latest phase of deformation. Thirdly, the Dombjerg Fault was a surface-breaching growth fault during the late Jurassic to early Cretaceous, and the exposed level in the hanging-wall was therefore at or near the surface at the time of faulting. The footwall, on the other hand, must have been deformed at deeper crustal levels during earlier tectonic phases. The footwall and hanging-wall have therefore had different depths of deformation and uplift histories during the latest deformational phase. The footwall may therefore have undergone more deformation prior to Jurassic-Cretaceous rifting, at greater depths, after which it has been uplifted and progressively fractured during later events. Although we are unable to differentiate the age of different structures observed in the damage zone, these are some of the options that may explain the contrasting footwall versus hanging-wall deformation observed.

Contrasting styles of deformation are also observed internally in the hanging-wall. The pervasively calcite-cemented CAZ is typified by faults, veins and a high frequency of joints, whereas the uncemented rocks outside CAZ were characterized predominantly by disaggregation zones, deformation bands and a low frequency of joints. These latter types of structures are associated with deformation of porous clastic rocks at shallow (less than 1 km) burial depths (e.g. Fisher and Knipe, 2001; Fossen et al., 2007). Conversely, the structures inside the cemented fault-proximal cementation and mineralization halo are typical for deformation in low-porous rocks, such as cemented clastic rocks. We infer that fault-related calcite cementation and mineralization must have occurred early during the Middle Jurassic – Early Cretaceous deformation, since the cementation and mineralization halo places a significant control on the distribution of these two distinct styles of fault-related deformation in the hanging-wall. The change in mechanical properties of the protolith within the CAZ in and around the fault causes further deformation to be genetically different from deformation that predates fault-related cementation and mineralization, or that occurs outside of the CAZ. The CAZ is thus considered to be a fault-related feature that is facilitated by fault-controlled fluid flow that controls further accommodation of mechanical deformation.

Calcite cementation can occur at near-surface depths at low temperatures (e.g. Bjørlykke, 1983), consistent with the fault being surface-breaching during the Late Jurassic-Early Cretaceous event. We therefore conclude that fault-related calcite cementation and mineralization occurred early on and at shallow depths during the Mesozoic faulting, and that it was facilitated by flow of fluids along the active Dombjerg Fault. There are several potential sources for the calcite, such as the underlying early rift succession of the Pelion and Payer Dal formations of the Middle to Late Jurassic Vardekløft Group (Alsgaard et al., 2003), or the Permian carbonates of the Foldvik Creek Group, which are locally preserved overlying crystalline rocks, below the Mesozoic rift-fill (Maync, 1947; Vischer, 1943; Surlyk and Korstgård, 2013).

5.3. Imaging syn-rift border faults in the subsurface

The studied fault exhibits an abundance of structures that can be studied in detail in outcrop (Fig. 11). This is not the case for similar faults in the sub-surface, which have economic importance in terms of their relevance in hydrocarbon exploration, but whose detailed structure is notoriously difficult to image on seismic data. Normal faults are generally too steep to be imaged in detail on seismic data, and their presence is therefore generally detected by the identification of discontinuous, displaced reflectors (lithologic layers). Seismic imaging of faults is also complicated by noise as the signal may be scattered and perturbed by the often steeply dipping faults (e.g. Hesthammer et al., 2001). This problem increases with

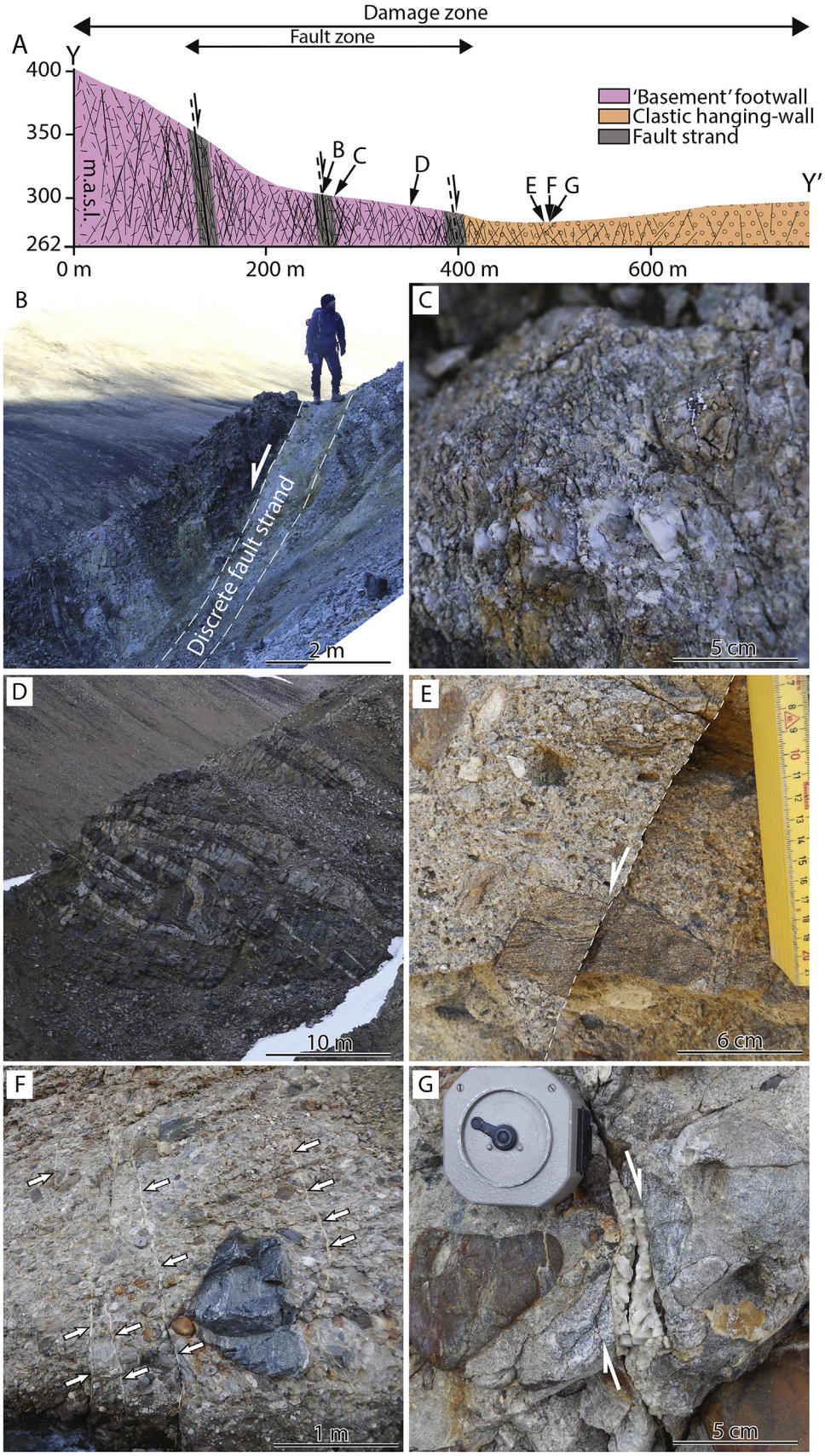

Fig. 10. Outcrop photopanel showing the variety of deformation found in transect B (marked Y-Y′ in Fig. 3) from footwall to hanging-wall across the fault zone. A) Transect topography and delineation of damage and central fault zone with marks for photograph localities. B) Discrete fault strand with c. 30 cm wide fault gouge zone and abundant fault breccias. C) Close-up of a fine-grained (clast size 2–4 mm) mosaic fault breccia. D) Intact but intensely fractured crystalline basement rocks in the footwall damage zone close to the fault core. E) Minor normal fault offsetting clasts in basinal conglomerate. F) Coarse-grained conglomerate with high fracture intensity, with some fractures displaying shear offset. G) Thick calcite fill with growth structures in a releasing bend of a normal-sense shear fracture, indicating the opening direction of the vein segment.

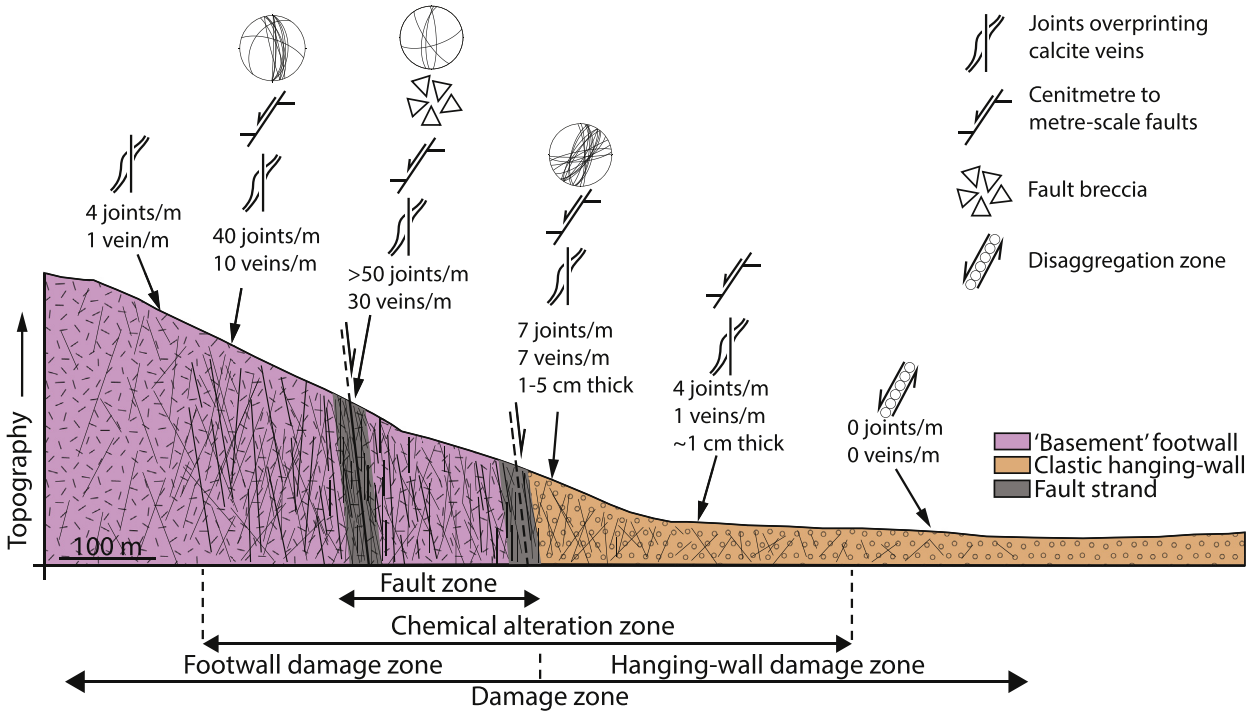

Fig. 11. Sketch transect summarizing observations across the Dombjerg Fault displaying the variation in deformation structures, orientations and fracture intensities.

the geometric complexity of faults, which may cause poor and chaotic fault imaging. Thick cover sequences and angular unconformities can also cause imaging problems as well as the nature of basin-bounding faults tendency to be at or beyond the edge of seismic reflection surveys based on the hydrocarbon industry focus on basins. Indeed, basin-bounding faults may form the coastline and thus neither appears in marine or onshore seismic surveys.

For comparison with the fault we studied in outcrop, we have selected two similar-scale subsurface examples of basin-bounding faults that juxtapose rift-related hanging-wall depocentres against crystalline basement footwalls (Fig. 13A and B). The Vesterdjupet Fault Zone bounds the North Træna Basin of the Norwegian rifted margin and juxtaposes Jurassic-Cretaceous rift climax clastics against Caledonian basement rocks with a maximum throw of 3.5 km accumulated through at least two phases of active rifting (Hansen et al., 2012; Henstra et al., 2015; Fig. 13A). The hydrocarbon-bearing Tanan sub-basin within the Tamtsag intracontinental rift basin in eastern Mongolia shows Jurassic-Cretaceous rift-related clastics juxtaposed against basement rocks across a rift shoulder border fault with up to 1800 m displacement (Zhou et al., 2014, Fig. 13B). Both examples show that, from analysis of the seismic data, one can interpret/estimate i) the cross-sectional trace of the basin-bounding fault, ii) seismic-scale segments, and iii) fault-related folding of the hanging-wall strata. It is not possible, however, to estimate the width of the damage zone, nor to draw out information about the detailed fault zone structure. There is, however, fault-parallel reflectivity in the immediate basement in the footwall of both faults, which could reflect footwall damage. Subtle fault-parallel reflections are seen along the bottom half of the basin-bounding fault in Fig. 13B, and we speculate that these may reflect fault-related fabric/damage. Along the Vesterdjupet Fault Zone (Fig. 13A), a c. 500 m wide zone of fault-parallel reflections in the footwall extends along the upper half of the fault zone. We interpret these reflections to be a multiple of the fault itself based on also observed seabed multiples and the fact that the spacing between the fault and the reflection equal the water-column. Multiples are thus also adding to the complexity of imaging faults and their damage zones with seismic data.

Although it may be possible to image some seismic-scale elements of a fault damage zone, perhaps by combining fault penetrating well-data with seismic attributes, its detailed structure is generally of a complexity and scale that is not observable at the scale of resolution provided by seismic data. These imaging-related limitations mean that an understanding of detailed fault structure in the subsurface cannot be based solely on seismic data, but must also include considerations based on information from boreholes (where available, e.g. Lin et al., 2007; Choi et al., 2016) and outcrop analogues, such as this study.

In addition to the imaging challenges associated with faults, there are issues related to interpretation that may cause a different kind of problem. Fault interpretations from seismic data are inherently deceptive, as they are commonly represented as thin lines on a seismic cross-section, and it may be tempting to treat faults as simple two-dimensional surfaces whereas they in reality are three-dimensional zones containing a range of sub-seismic structures. In fact, faults are routinely treated as 2D objects in reservoir models, which may further contribute to misguiding interpreters to think that faults are simple structures (Fredman et al., 2008; Braathen et al., 2009). Knowledge about structural geology and the use of outcrop analogues are therefore crucial to understanding the sub-seismic structure of faults, and furthermore to assess and understand their flow properties.

5.4. Understanding the flow properties of syn-rift border faults in the subsurface

The Dombjerg Fault provides an example that may illuminate what can be expected from syn-rift border faults in the subsurface. The juxtaposition of the porous reservoir rocks against low permeable ('tight') crystalline metamorphic basement rocks is a typical trap configuration in syn-rift hydrocarbon plays that depend on lateral fault seal (Fig. 14). As seen here, such faults may comprise

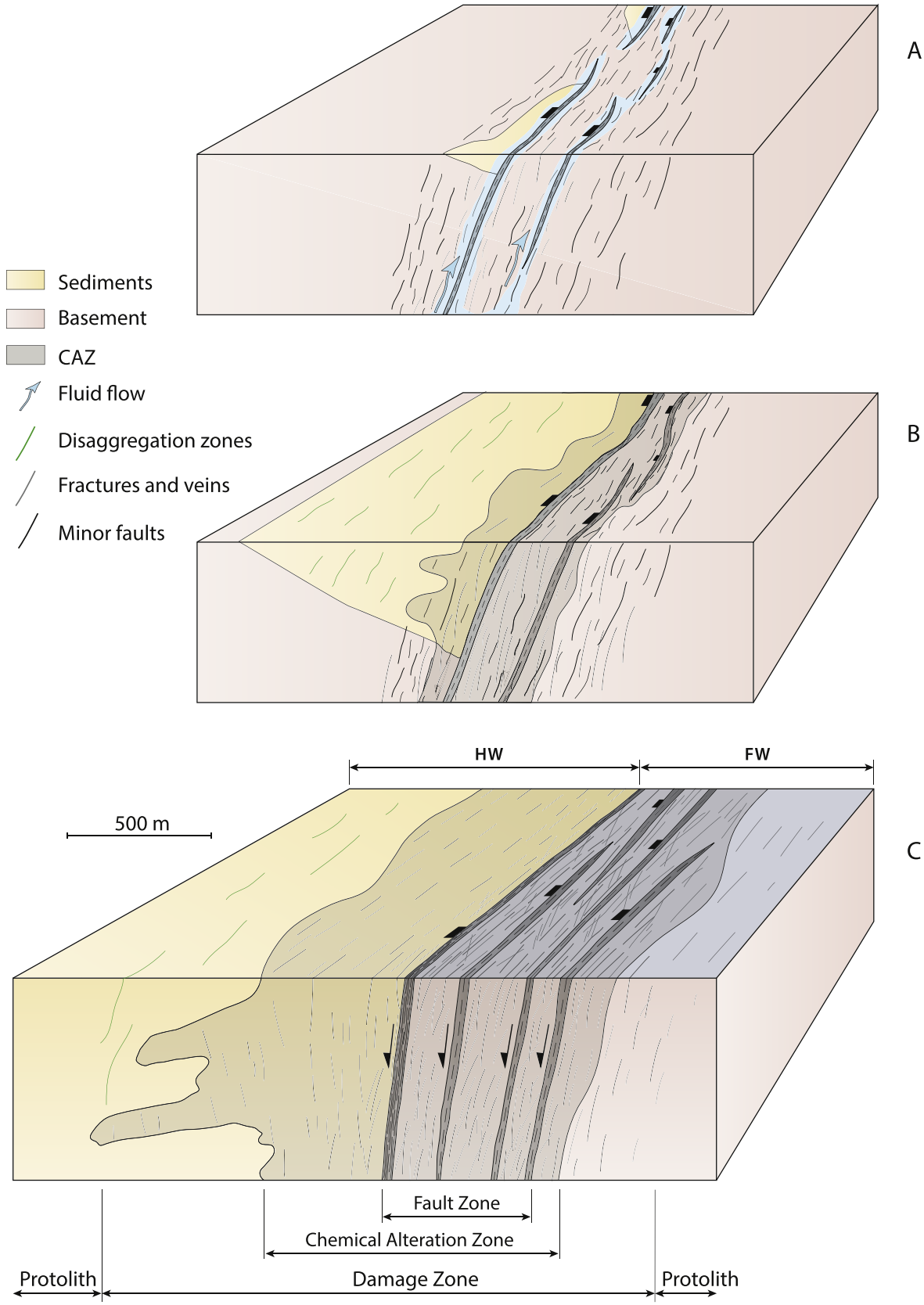

Fig. 12. Schematic 3D block diagrams showing the conceptual fault development. A) incipient faulting and associated fluid flow within the fault zone. B) CAZ controls type of deformation during later deformation. C) The width of the CAZ varies both vertically and along strike of the fault zone both in the footwall (FW) and hanging-wall (HW).

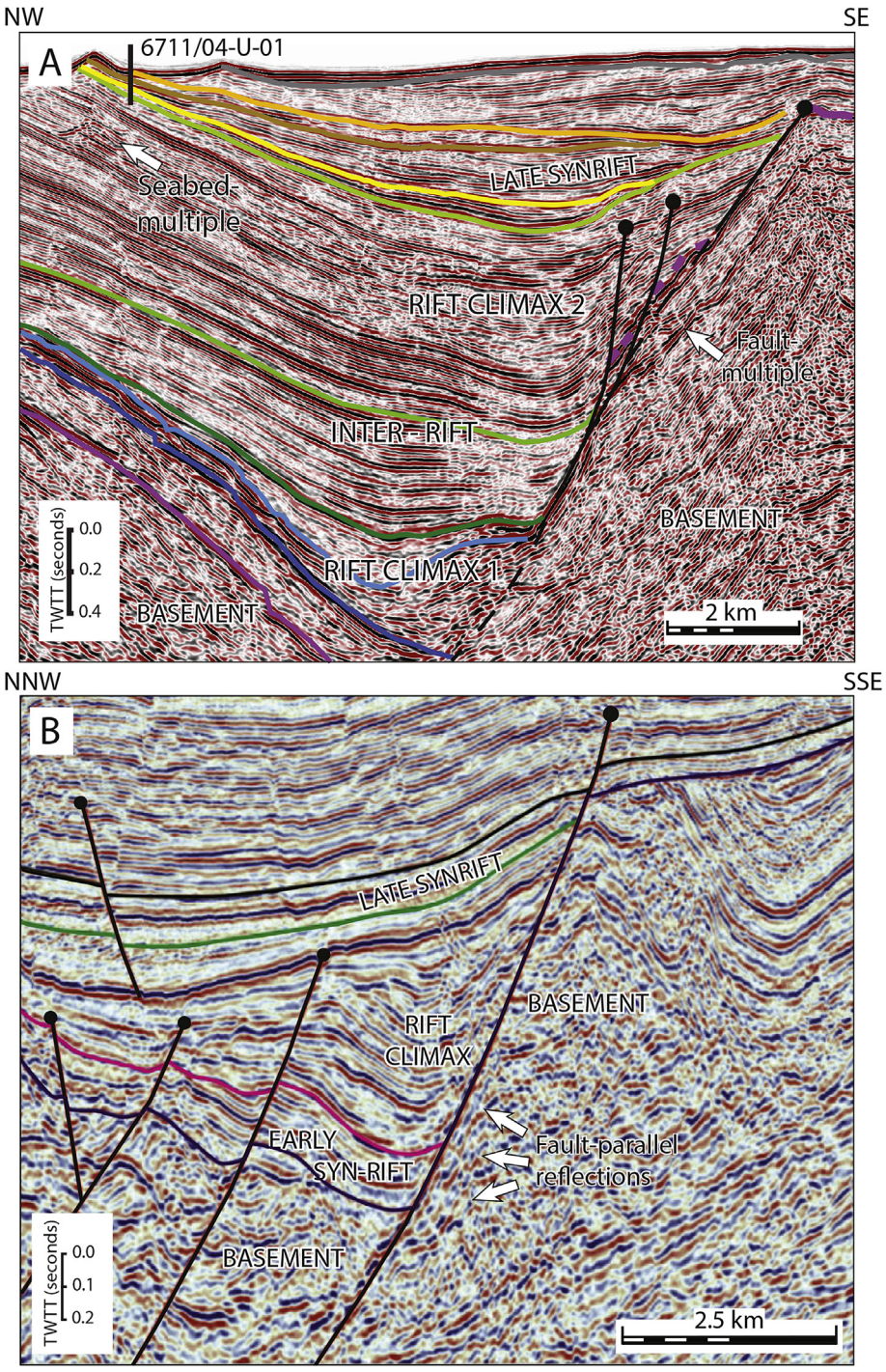

Fig. 13. Seismic analogues for the Wollaston Forland area and the Dombjerg Fault. A) The Vesterdjupet Fault, offshore Lofoten, Norway (modified after Henstra et al., 2015) displaying fault parallel reflections in the footwall. B) The Tanan Basin in eastern Mongolia (modified after Zhou et al., 2014) displaying fault parallel reflections in the footwall.

flow-reducing structures, (e.g. low-permeable fault rock assemblages, veins and fault-related cementation in the CAZ) as well as features that provide conduits for fluid flow (e.g. joints). This may lead to (i) anisotropic flow properties, where cross-fault flow is retarded, but where along fault-flow is facilitated; (ii) a risk of compromising the lateral fault seal by up-fault leakage along open fractures (joints and slip surfaces); and (iii) a risk of compromising top seal for the same reasons.

Another aspect to consider when discussing flow properties is the timing of different structures. Veins in the fault zone are considered to pre-date or be synchronous with cementation and are probably sealing after they were mineralized. The vein fill is proof that, at one point in their evolution, they were open fractures and fluid conduits. The timing of vein mineralization in relation to hydrocarbon migration would therefore be an important factor to consider in the sense that these fractures would provide an up-fault conduit for escape of hydrocarbons prior to mineralization. The uncemented joints, which postdate cementation and veins, would also function as up-fault conduits for hydrocarbon escape, and thus the timing of jointing is also an important factor. The joints are

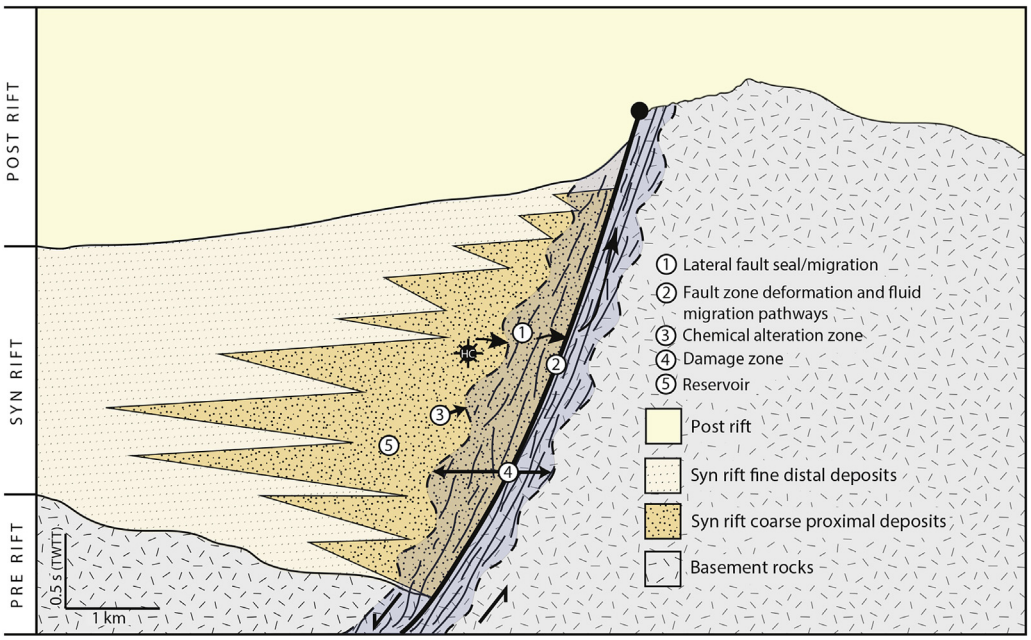

Fig. 14. Schematic setting of a basement bounded border-fault with a syn-rift depocentre filled with potential reservoir clastics.

located in the CAZ and are interpreted based on frequency increase towards the fault zone to be mainly related to fault movement, but may also include a component of late features related to uplift and exhumation.

Another aspect of fault related fluid flow is that, within the CAZ, reservoir/aquifer properties are adversely affected by cementation, and may cause a near-complete loss of porosity and permeability (Fig. 14). This affects not only flow properties, but, depending on the rock volume occupied by the CAZ, may significantly reduce volumes in hydrocarbon prospects or fields.

In summary, understanding the relationships and timing of mechanical damage and chemical alteration around the fault is highly important to better understand the type of structures to be expected in the subsurface, and therefore highly important also for any attempt to predict flow properties. Such understanding does not come from standard types of analyses, such as analysis of juxtaposition diagrams, estimation of shale gouge ratio or shale smear potential, but should be based on careful analysis of available information about lithology, mineralogy, diagenesis, tectonic history, depth of deformation, thermal history, geochemistry and more. Often much of this information may not be available, and even if it is, part of the exercise rests on a foundation of geological experience, educated guesswork, and luck. Therefore, studying outcrop analogues, such as the example presented in this study, is important to expand the global experience pool, which may help geologists predict the ever-enigmatic subsurface. A final point is that when selecting well placements near faults, the possibility of drilling into the CAZ must be considered, as it could lead to failure in detecting sufficient-quality reservoir rocks further away from the fault, and failed well tests due to inability to mobilize any hydrocarbons present within the low-permeable CAZ.

6. Conclusions

Our qualitative analysis of the structure of an exposed basin-bounding fault gives new insights into the tectonic boundaries between 'basement' and rift-sequence rocks, highlighting an often underreported interplay in space and time between fault-related chemical alteration (mineralization and cementation) and mechanical damage. The most significant observations, conclusions and implications of this study are:

- Syn-rift border faults with km-scale displacement may be associated with up to km-scale damage zones, which include a range of structures that generally fall below seismic resolution. Such structures may include discrete fault strands, fault rock assemblages, veins, joints, deformation bands and chemical fluid-rock interactive products such as pervasive cementation and mineralization.
- We suggest that future studies of fault damage zones with associated fault related cementation and mineralization adopt the use of 'chemical alteration zone' (CAZ) to describe the zone of chemically altered protolith around a fault. Including chemical alteration associated with faults within fault models will help highlight relationships between chemical alteration and mechanical damage.
- The CAZ is controlled by fluid flow related to faulting and mechanical damage (e.g. by flow along fractures to form veins). Equally, once formed, the CAZ affects rock and reservoir properties, and may control the distribution and form of further mechanical damage. Elucidating the (relative) timing, depth and temperature of chemical and mechanical damage during faulting is therefore key in determining the structural style and flow properties of any fault zone.
- For syn-rift border faults juxtaposing syn-rift clastics with basement rocks, significant differences in deformation between the footwall and the hanging-wall is to be expected. Deformation in hanging-wall sedimentary rocks may include chemical alteration and associated porosity loss, as well as mechanical damage in the form of faults, veins, joints and deformation bands. Footwall deformation may include chemical alteration such as mineralization, and mechanical damage such as faults, veins and joints. The footwall and hanging-wall damage zones will also have contrasting flow properties.
- The structure of the 'central fault zone' (*sensu* Childs et al., 2009) should in general be expected to exhibit more complexity than

that suggested by a single 'fault core' scheme (*sensu* Caine et al., 1996). Given the amount of displacement generally accommodated by basin-bounding rift-related faults (commonly on the scale of several hundred metres to kilometres), slip may instead be distributed onto a series of discrete fault strands, as seen in the Dombjerg fault zone and as suggested by e.g. Faulkner et al. (2010), with each strand associated with individual assemblages of fault rock, or 'fault cores'.

- Any attempt to forecast flow properties of syn-rift border faults must consider that flow-impeding and flow-enhancing mechanical damage as well as chemical alteration may co-exist within a fault damage zone, which may lead to anisotropic flow properties. In order to make predictions about fluid flow in a hydrocarbon context, understanding the relative timing of deformation, chemical alteration and hydrocarbon migration is key.
- Cementation and porosity reduction within the CAZ may reduce the flow properties and volumes of any reservoir or aquifer. This should be taken under consideration when calculating reservoir/aquifer size or economic viability, and would be very important when determining well placements. For example, drilling a hydrocarbon exploration well within the CAZ could result in failure to test an otherwise viable prospect, or sample a fault-proximal cemented interval that would misrepresent the overall reservoir properties further away from the fault.

Our study documents the interplay between chemical alteration and mechanical damage, and this may be extended to any type of fault. Examples of other types of CAZs include fault-controlled dolomites (e.g. Davies and Smith, 2006; Sharp et al., 2010), fault-controlled stalactites (e.g. Kim and Sanderson, 2010), fault-controlled travertine deposits (e.g. Dockrill and Shipton, 2010) and fault-controlled hydrothermal silicification (Glen, 1987). We therefore suggest that the term 'CAZ' be used to describe all fault zones that have undergone a combination of chemical alteration and mechanical damage. A stronger focus on the interplay between chemical and mechanical processes in space and time will lead to an improved understanding of the structure, evolution and flow properties of fault zones.

Acknowledgements

We thank Norske Shell for funding of the 2014 Wollaston Forland field work as well as the first author's PhD project. The WOLLGAN project group, and in particular Erik P. Johannessen and Johan Petter Nystuen, are thanked for helpful discussions and insights that significantly helped our field campaign. Arild Andresen is thanked for invaluable help with planning, logistics and equipment for the 2014 expedition to Wollaston Forland, as well as for sharing his wide knowledge of Greenland geology. The Ministry of Environment and Nature of the government of Greenland is thanked for allowing access to the Northeast Greenland National Park for fieldwork conducted under KNNO expedition permit C-14-14. Funding for S.-A. Grundvåg and I. Midtkandal's participation in this work was provided by the LoCrA project (Lower Cretaceous clastic wedges, an under-explored play in the Arctic), initiated within the FORCE consortium. S.-A. Grundvåg also received funding from the ARCEx project (Research Centre for Arctic Petroleum Exploration) which is funded by the Research Council of Norway (grant number 228107). Leif-Erik Rydland Pedersen is thanked for help with thinsection analysis. Haakon Fossen is thanked for helpful discussions. Eva Bjørseth at the Department of Earth Science, UiB, is gratefully acknowledged for drafting Fig. 12. Constructive and insightful comments from Nigel Woodcock, Eiichi Ishii, Andrea Billi, one anonymous reviewer as well by Editor Toru Takeshita, have led to significant improvements of the final version of this paper.

References

Alsgaard, P.C., Felt, V.L., Vosgerau, H., Surlyk, F., 2003. The Jurassic of Kuhn Ø, North-East Greenland. The Jurassic of Denmark and Greenland. Geol. Surv. Den. Greenl. Bull. 1, 865–892.
Bastesen, E., Braathen, A., Nøttveit, H., Gabrielsen, R.H., Skar, T., 2009. Extensional fault cores in micritic carbonate – case studies from the Gulf of Corinth, Greece. J. Struct. Geol. 31, 403–420.
Billi, A., Salvini, F., Storti, F., 2003. The damage zone-fault core transition in carbonate rocks: implications for fault growth, structure and permeability. J. Struct. Geol. 25, 1779–1794.
Bjørlykke, K., 1983. Diagenetic reactions in sandstones. In: Parker, A., Sellwood, B.W. (Eds.), Sediment Diagenesis. Springer Netherlands, pp. 169–213.
Braathen, A., Tveranger, J., Fossen, H., Skar, T., Cardozo, N., Semshaug, S.E., Bastesen, E., Sverdrup, E., 2009. Fault facies and its application to sandstone reservoirs. AAPG Bull. 93, 891–917.
Caine, J.S., Bruhn, R.L., Forster, C.B., 2010. Internal structure, fault rocks, and inferences regarding deformation, fluid flow, and mineralization in the seismogenic Stillwater normal fault, Dixie Valley, Nevada. J. Struct. Geol. 32, 1576–1589.
Caine, J.S., Evans, J.P., Forster, C.B., 1996. Fault zone architecture and permeability structure. Geology 24, 1025–1028.
Chan, M.A., Parry, W., Bowman, J., 2000. Diagenetic hematite and manganese oxides and fault-related fluid flow in Jurassic sandstones, southeastern Utah. AAPG Bull. 84, 1281–1310.
Chester, F.M., Logan, J.M., 1986. Implications for mechanical properties of brittle faults from observations of the Punchbowl fault zone, California. Pure Appl. Geophys. 124, 79–106.
Childs, C., Manzocchi, T., Walsh, J.J., Bonson, C.G., Nicol, A., Schöpfer, M.P., 2009. A geometric model of fault zone and fault rock thickness variations. J. Struct. Geol. 31, 117–127.
Childs, C., Walsh, J.J., Watterson, J., 1997. Complexity in fault zone structure and implications for fault seal prediction. Nor. Pet. Soc. Spec. Publ. 7, 61–72.
Choi, J.H., Edwards, P., Ko, K., Kim, Y.S., 2016. Definition and classification of fault damage zones: a review and a new methodological approach. Earth Sci. Rev. 152, 70–87.
Christiansen, F., Larsen, H., Marcussen, C., Hansen, K., Krabbe, H., Larsen, L., Piasecki, S., Stemmerik, L., Watt, S., 1992. Uplift study of the Jameson Land basin, East Greenland. Nor. J. Geol. 72, 291–294.
Coward, M., Dewey, J., Hempton, M., Holroyd, J., 2003. Tectonic Evolution. In: Evans, D., Graham, C., Armour, A., Bathurst, P. (Eds.), The Millennium Atlas: Petroleum Geology of the Central and Northern North Sea. The Geological Society of London, pp. 17–33.
Cowie, P.A., Shipton, Z.K., 1998. Fault tip displacement gradients and process zone dimensions. J. Struct. Geol. 20, 983–997.
Dallmeyer, R., Strachan, R., Henriksen, N., 1994. 40Ar/39Ar mineral age record in NE Greenland: implications for tectonic evolution of the North Atlantic Caledonides. J. Geol. Soc. 151, 615–628.
Davies, G.R., Smith, L.B., 2006. Structurally controlled hydrothermal dolomite reservoir facies: an overview. Am. Assoc. Petroleum Geol. Bull. 90, 1641–1690.
De Joussineau, G., Aydin, A., 2007. The evolution of the damage zone with fault growth in sandstone and its multiscale characteristics. J. Geophys. Res. 112.
Dietz, R.S., Holden, J.C., 1970. Reconstruction of Pangaea: breakup and dispersion of continents, Permian to present. J. Geophys. Res. 75, 4939–4956.
Dockrill, B., Shipton, Z.K., 2010. Structural controls on leakage from a natural CO^2 geologic storage site: central Utah, USA. J. Struct. Geol. 32, 1768–1782.
Doré, A., Lundin, E., Jensen, L., Birkeland, Ø., Eliassen, P., Fichler, C., 1999. Principal tectonic events in the evolution of the northwest European Atlantic margin. In: Fleet, A.J., Boldy, S.A. (Eds.), Petroleum Geology of Northwest Europe, Proceedings of the 5th Conference. Geological Society of London, pp. 41–61.
Evans, J.P., Forster, C.B., Goddard, J.V., 1997. Permeability of fault-related rocks, and implications for hydraulic structure of fault zones. J. Struct. Geol. 19, 1393–1404.
Faleide, J.I., Bjørlykke, K., Gabrielsen, R.H., 2010. Geology of the Norwegian continental Shelf. In: Bjørlykke, K. (Ed.), Petroleum Geoscience: from Sedimentary Environments to Rock Physics. Springer-Verlag, Berlin Heidelberg, pp. 467–499.
Faulkner, D., Jackson, C., Lunn, R., Schlische, R., Shipton, Z., Wibberley, C., Withjack, M., 2010. A review of recent developments concerning the structure, mechanics and fluid flow properties of fault zones. J. Struct. Geol. 32, 1557–1575.
Faulkner, D., Lewis, A., Rutter, E., 2003. On the internal structure and mechanics of large strike-slip fault zones: field observations of the Carboneras fault in southeastern Spain. Tectonophysics 367, 235–251.
Fisher, D.M., Brantley, S.L., 1992. Models of quartz overgrowth and vein formation: deformation and episodic fluid flow in an ancient subduction zone. J. Geophys. Res. 97, 20,043–20,061.
Fisher, Q.J., Knipe, R.J., 2001. The permeability of faults within siliciclastic petroleum reservoirs of the North Sea and Norwegian Continental Shelf. Mar. Petroleum Geol. 18, 1063–1081.
Fodor, L., Turki, S., Dalub, H., Al Gerbi, A., 2005. Fault-related folds and along-dip segmentation of breaching faults: syn-diagenetic deformation in the south-

western Sirt basin, Libya. Terra nova.. 17, 121–128.
Fossen, H., Rotevatn, A., 2016. Fault linkage and relay structures in extensional settings – a review. Earth Sci. Rev. 154, 14–28.
Fossen, H., Schultz, R.A., Rundhovde, E., Rotevatn, A., Buckley, S.J., 2010. Fault linkage and graben step overs in the Canyonlands (Utah) and the North Sea Viking Graben, with implications for hydrocarbon migration and accumulation. Am. Assoc. Petroleum Geol. Bull. 94, 597–613.
Fossen, H., Schultz, R.A., Shipton, Z.K., Mair, K., 2007. Deformation bands in sandstone: a review. J. Geol. Soc. 164, 755–769.
Fredman, N., Tveranger, J., Cardozo, N., Braathen, A., Soleng, H., Roe, P., Skorstad, A., Syversveen, A.R., 2008. Fault facies modeling: technique and approach for 3-D conditioning and modeling of faulted grids. AAPG Bull. 92, 1457–1478.
Gawthorpe, R., Leeder, M., 2000. Tectono-sedimentary evolution of active extensional basins. Basin Res. 12, 195–218.
Gee, D.G., Fossen, H., Henriksen, N., Higgins, A.K., 2008. From the early Paleozoic platforms of Baltica and Laurentia to the Caledonide orogen of Scandinavia and Greenland. Episodes 31, 44–51.
Glen, R., 1987. Copper-and gold-rich deposits in deformed turbidites at Cobar, Australia; their structural control and hydrothermal origin. Econ. Geol. 82, 124–140.
Gomila, R., Arancibia, G., Mitchell, T.M., Cembrano, J.M., Faulkner, D.R., 2016. Palaeopermeability structure within fault-damage zones: a snap-shot from microfracture analyses in a strike-slip system. J. Struct. Geol. 83, 103–120.
Hansen, J.A., Bergh, S.G., Henningsen, T., 2012. Mesozoic rifting and basin evolution on the Lofoten and Vesterålen Margin, North-Norway; time constraints and regional implications. Nor. J. Geol. 91, 203–228.
Hartz, E., Andresen, A., Martin, M., Hodges, K., 2000. U–Pb and 40Ar/39Ar constraints on the Fjord region detachment zone: a long-lived extensional Fault in the central East Greenland Caledonides. J. Geol. Soc. Lond. 157, 795–809.
Henstra, G.A., Rotevatn, A., Gawthorpe, R.L., Ravnås, R., 2015. Evolution of a major segmented normal fault during multiphase rifting: the origin of plan-view zigzag geometry. J. Struct. Geol. 74, 45–63.
Henstra, G.A., Grundvåg, S.-A., Johannessen, E.P., Kristensen, T.B., Midtkandal, I., Nystuen, J.P., Rotevatn, A., Surlyk, F., Sæther, T., Windelstad, J., 2016. Depositional processes and stratigraphic architecture within a coarse-grained rift-margin turbidite system: the Wollaston Forland Group, east Greenland. Mar. Petroleum Geol. 76, 187–209.
Hesthammer, J., Landrø, M., Fossen, H., 2001. Use and abuse of seismic data in reservoir characterisation. Mar. Petroleum Geol. 18, 635–655.
Johansen, T.E.S., Fossen, H., Kluge, R., 2005. The impact of syn-faulting porosity reduction on damage zone architecture in porous sandstone: an outcrop example from the Moab Fault, Utah. J. Struct. Geol. 27, 1469–1485.
Kalsbeek, F., 1995. Geochemistry, tectonic setting, and poly-orogenic history of Palaeoproterozoic basement rocks from the Caledonian fold belt of North-East Greenland. Precambrian Res. 72, 301–315.
Kim, Y.S., Peacock, D.C.P., Sanderson, D.J., 2003. Mesoscale strike-slip faults and damage zones at Marsalforn, Gozo Island, Malta. J. Struct. Geol. 25, 793–812.
Kim, Y.S., Peacock, D.C.P., Sanderson, D.J., 2004. Fault damage zones. J. Struct. Geol. 26, 503–517.
Kim, Y.S., Sanderson, D., 2010. Inferred fluid flow through fault damage zones based on the observation of stalactites in carbonate caves. J. Struct. Geol. 32, 1305–1316.
Knipe, R.J., 1992. Faulting processes and fault seal. In: Larsen, R.M., Brekke, H., Larsen, B.T., Talleraas, E. (Eds.), Structural and Tectonic Modelling and its Application to Petroleum Geology, pp. 325–342. Norwegian Petroleum Society Special Publication 1.
Knipe, R.J., Jones, G., Fisher, Q.J., 1998. Faulting, fault sealing and fluid flow in hydrocarbon reservoirs: an introduction. In: Jones, G., Fisher, Q.J., Knipe, R.J. (Eds.), Faulting, Fault Sealing and Fluid Flow in Hydrocarbon Reservoirs. Geological Society, London. Special Publications 147, vii-xxi.
Larsen, P.H., 1988. Relay structures in a Lower Permian basement-involved extension system, East Greenland. J. Struct. Geol. 10, 3–8.
Laubach, S.E., Eichhubl, P., Hilgers, C., Lander, R.H., 2010. Structural diagenesis. J. Struct. Geol. 32, 1866–1872.
Lin, A., Maruyama, T., Kobayashi, K., 2007. Tectonic implications of damage zone-related fault-fracture networks revealed in drill core through the Nojima fault, Japan. Tectonophysics 443, 161–173.
Maync, W., 1947. Stratigraphie der Jurabildungen Ostgronlands, zwischen Hochstetterbugten (75°N.) und dem Kejser Franz Joseph Fjord (73°N.). Meddelelser Om. Grønl. 132, 1–223.
Maync, W., 1949. The Cretaceous beds between Kuhn island and Cape Franklin (Gauss Peninsula), northern East Greenland. Meddelelser Om. Grønl. 133, 1–291.
McClelland, W.C., Gilotti, J.A., 2003. Late-stage extensional exhumation of high-pressure granulites in the Greenland Caledonides. Geology 31, 259–262.
Michie, E.A.H., Haines, T.J., Healy, D., Neilson, J.E., Timms, N.E., Wibberley, C.A.J., 2014. Influence of carbonate facies on fault zone architecture. J. Struct. Geol. 65, 82–99.
Murray, R.C., 1960. Origin of porosity in carbonate rocks. J. Sediment. Res. 30, 59–84.
Noe-Nygaard, A., 1976. Tertiary igneous rocks between Shannon and Scoresby Sund, East Greenland. In: Escher, A., Watt, W.S. (Eds.), Geology of Greenland. Geological Survey of Greenland, pp. 386–402.
Ord, D., Clemmey, H., Leeder, M., 1988. Interaction between faulting and sedimentation during Dinantian extension of the Solway basin, SW Scotland. J. Geol. Soc. 145, 249–259.
Peacock, D.C.P., 2008. Architecture, gods and gobbledygook. J. Struct. Geol. 30, 687–688.
Price, S., Brodie, J., Whitham, A., Kent, R., 1997. Mid-tertiary rifting and magmatism in the Traill Ø region, East Greenland. J. Geol. Soc. 154, 419–434.
Ravnås, R., Steel, R.J., 1998. Architecture of marine rift-basin successions. Am. Assoc. Petroleum Geol. Bull. 82, 110–146.
Scholz, C.H., 2002. The Mechanics of Earthquakes and Faulting. Cambridge University Press, 471 pp.
Sharp, I., Gillespie, P., Morsalnezhad, D., Taberner, C., Karpuz, R., Vergés, J., Horbury, A., Pickard, N., Garland, J., Hunt, D., 2010. Stratigraphic architecture and fracture-controlled dolomitization of the Cretaceous Khami and Bangestan groups: an outcrop case study, Zagros Mountains, Iran. In: Van Buchem, F.S.P., Gerdes, K.D., Esteban, M. (Eds.), Mesozoic and Cenozoic Carbonate Systems of the Mediterranean and the Middle East: Stratigraphic and Diagenetic Reference Models. Geological Society, London, pp. 343–396. Special Publications 329.
Sharp, I.R., Gawthorpe, R.L., Underhill, J.R., Gupta, S., 2000. Fault-propagation folding in extensional settings: examples of structural style and synrift sedimentary response from the Suez rift, Sinai, Egypt. Geol. Soc. Am. Bull. 112, 1877–1899.
Shipton, Z.K., Cowie, P.A., 2001. Damage zone and slip-surface evolution over μm to km scales in high-porosity Navajo sandstone, Utah. J. Struct. Geol. 23, 1825–1844.
Shipton, Z.K., Cowie, P.A., 2003. A conceptual model for the origin of fault damage zone structures in high-porosity sandstone. J. Struct. Geol. 25, 333–344.
Sibson, R.H., 1977. Fault rocks and fault mechanisms. J. Geol. Soc. Lond. 133, 191–213.
Spencer, A.M., Larsen, V.B., 1990. Fault traps in the northern North Sea. Geol. Soc. Lond. Spec. Publ. 55, 281–298.
Surlyk, F., 1978. Submarine fan sedimentation along fault scarps on tilted fault blocks: (Jurassic-Cretaceous boundary, East Greenland). Bull. Grønl. Geol. Unders. 128, 1–108.
Surlyk, F., 1984. Fan-delta to submarine fan conglomerates of the Volgian-Valanginian Wollaston forland group, east Greenland. In: Koster, E.H., Steel, R.J. (Eds.), Sedimentology of Gravels and Conglomerates. Canadian Society of Petroleum Geology, pp. 359–382. Memoir 10.
Surlyk, F., 1990. A Jurassic sea-level curve for East Greenland. Palaeogeogr. Palaeoclimatol. Palaeoecol. 78, 71–85.
Surlyk, F., 2003. The Jurassic of East Greenland: a sedimentary record of thermal subsidence, onset and culmination of rifting. Geol. Surv. Den. Greenl. Bull. 1, 659–722.
Surlyk, I., Clemmensen, L.B., 1983. Rift propagation and eustacy as controlling factors during Jurassic inshore and shelf sedimentation in northern East Greenland. Sediment. Geol. 34, 119–143.
Surlyk, F., Clemmensen, L.B., Larsen, H.C., 1981. Post-Paleozoic evolution of the East Greenland continental margin. In: Kerr, J.W., Ferguson, A.J. (Eds.), Geology of the North Atlantic Borderlands, pp. 611–645. Canadian Society of Petroleum Geologists Memoir 7.
Surlyk, F., Hurst, J., Piasecki, S., Rolle, F., Scholle, P., Stemmerik, L., Thomsen, E., 1986. The Permian of the western margin of the Greenland Sea – a future exploration target. In: Halbouty, M.T. (Ed.), Future Petroleum Provinces of the World, pp. 629–659. Memoir of the American Association of Petroleum Geologists 40.
Surlyk, F., Korstgård, J., 2013. Crestal unconformities on an exposed Jurassic tilted fault block, Wollaston Forland, East Greenland as an analogue for buried hydrocarbon traps. Mar. Petroleum Geol. 44, 82–95.
Sutherland, R., Toy, V.G., Townend, J., Cox, S.C., Eccles, J.D., Faulkner, D.R., Prior, D.J., Norris, R.J., Mariani, E., Boulton, C., Carpenter, B.M., Menzies, C.D., Little, T.A., Hasting, M., De Pascale, G.P., Langridge, R.M., Scott, H.R., Reid Lindroos, Z., Fleming, B., Kopf, A.J., 2012. Drilling reveals fluid control on architecture and rupture of the Alpine fault, New Zealand. Geology 40, 1143–1146.
Tarasewicz, J.P.T., Woodcock, N.H., Dickson, J.A.D., 2005. Carbonate dilation breccias: examples from the damage zone to the Dent Fault, northwest England. Geol. Soc. Am. Bull. 117, 736–745.
Vischer, A., 1943. Die postdevonische tectonic von ostgrönland zwischen 74° und 75°N. Br., Kuhn Ø, Wollaston Forland, Clavering Ø und angrenzende gebiete. Meddelelser Om. Grønl. 133, 1–195.
Woodcock, N.H., Mort, K., 2008. Classification of fault breccias and related fault rocks. Geol. Mag. 145, 435–440.
Woodcock, N.H., Dickson, J.A.D., Tarasewicz, J.P.T., 2007. Transient fracture permeability and reseal hardening in fault zones: evidence from dilation breccia textures. In: Lonergan, L., Jolly, R.J.H., Rawnsley, K., Sanderson, D.J. (Eds.), Fractured Reservoirs. Geological Society, London, pp. 43–53. Special Publication 270.
Woodcock, N.H., Sayers, N.J., Dickson, J.A.D., 2008. Fluid flow history from damage zone cements near the Dent and Rawthey faults, NW England. J. Geol. Soc. Lond. 165, 829–837.
Zhou, Y., Ji, Y., Pigott, J.D., Meng, Q.A., Wan, L., 2014. Tectono-stratigraphy of Lower Cretaceous Tanan sub-basin, Tamtsag Basin, Mongolia: sequence architecture, depositional systems and controls on sediment infill. Mar. Petroleum Geol. 49, 176–202.
Ziegler, P.A., 1988. Evolution of the Arctic-North Atlantic and the Western Tethys. Am. Assoc. Petroleum Geol. Mem. 43, 164–196.